14

PERTURBATIVE QUANTUM CHROMODYNAMICS IN A CAVITY

By A J Stoddart

Submitted in partial fulfillment
of the requirements for
the degree of
Master of Science
in Theoretical Physics
at the University of Cape Town 1987
Supervised by Prof R D Viollier

INDEX

0 ABSTRACT

BRS invariant Quantum Chromodynamics is quantized in a static spherical cavity, subject to the boundary conditions of the MIT group. Using the Gell-Mann and Low theorem and a modified version of Goldstones theorem we formulate perturbation theory. In 4th order perturbation theory we calculate the Feynman diagrams corresponding to configuration mixing and two gluon annihilation. The results are inserted into the MIT bag model and compared with hadron spectra.

1 INTRODUCTION

It is believed that Quantum Chromodynamics (QCD) describes the strong interactions of quarks and gluons. At high energies, because the running coupling constant is small and perturbation theory may be applied, the theory has been relatively successful in describing hadronic physics. At low energies there has been little success in understanding hadronic physics from the fundamentals of QCD and it is clear that an understanding of the vacuum is essential.

The experimentally observed property of confinement restricts the colour carrying constituents of hadrons to a small volume. In the absence of a theoretical pathway from QCD in infinite space to this situation, our approach is simply to study QCD in a small volume.

Subsequent to the MIT bag model, the task of formulating perturbative QCD in a cavity has been pursued by (Le 79, Cl 80, Ha 83). A recent effort (Bu 83, Zi 86, Bu 86) has developed an elegant, rigorous and convenient version of perturbative QCD in a static spherical cavity. Another recent paper (Go 86), based on the multiple reflection formalism (Ha 83), has satisfactorily concluded a series of attempts to regularise the lowest order self-energy of the $1s1/2$ quark in the cavity. However the problem of the gluon self-energy is still outstanding, and a practical renormalization program will be necessary, before cavity field theory will be able to tackle bound states in a thorough way.

Our intention is to use the formalism of (Zi 86) to take our understanding of cavity QCD a little further. We calculate 4th order diagrams in perturbation theory, specifically those non-divergent graphs that give rise to configuration mixing, and those responsible for two gluon annihilation. As far as we know, the results for configuration mixing are new. The results for two gluon annihilation were obtained independently of (Do 83), which we discovered subsequent to our calculation.

We do not intend to consider our results in the context of the many models and parameterizations of baryon spectroscopy on the market (Fl 84, Ca 83). However we feel it to be useful to consider our results in the context of at least one such model.

We therefore rely on the MIT bag model (Ch 74, de 75) to give a connection between QCD in a cavity and the experimental hadron spectra. It is unfortunate that we have to rely on such a phenomenological model, but, independently of this, the techniques and the results provide valuable experience in dealing with such a small volume field theory. In the meantime we have provided interesting information in the framework of the MIT bag model.

In the original MIT bag model the second order perturbative QCD corrections are used to generate the hyperfine splittings. A wide variety of other models have since been proposed. However the perturbative calculation of further QCD corrections in the MIT bag has not progressed far in the ten years of the models existence.

The reason for this lies largely in the difficult nature of the calculations. They involve numerous radial integrals, complicated angular momentum factors, and finally tedious mode sums, paying attention to selection rules.

Given the large value of the strong coupling constant, it is important to consider the effect of higher order corrections. Only one author (Do 83) seems to have tackled this task, for the case of two gluon annihilation in pseudoscalar mesons. (Ba 84) has, in a calculation of the Coulomb spike effect, implicitly included higher order corrections (in a non-perturbative way). (Ge 86) have performed ladder sums in mesons with a full dynamical treatment of the gluon.

Our goal in this thesis will be to calculate 4th order perturbative effects. The exercise is undertaken primarily to understand the trends that emerge for two (anti)quark states interacting in their lowest cavity mode. A parallel objective is to understand

the practical difficulties of such calculations, as an example of higher order cavity perturbation theory in general.

The framework of this thesis is as follows. In section 2 we briefly introduce gauge theories, specifically Chromodynamics. We then canonically quantize the theory in a covariant way. To do so we have to introduce a new type of gauge invariance, the Becchi-Rouet-Stora gauge invariance (Be 74, Be 76). We do not attempt a full discussion of this topic, but rather sketch the outline and some details insofar as they are necessary to our specific calculation.

In section 3 we introduce the interaction picture and Gell-Mann and Low theorem. This is standard, but in addition we discuss the case of degenerate states, and Goldstone's theorem. Recognizing that when dealing with states other than the vacuum, Goldstones theorem no longer applies, we derive a modified version of Goldstone's theorem.

In section 4 we look at the cavity boundary conditions, which are chosen to be those of the MIT group, and the consequential quark and gluon cavity modes. We write down the field operators and propagators in terms of the cavity modes.

In section 5 we calculate the second order perturbation shift of a two quark system as an example. We then proceed to formally calculate the 4th order diagram that is responsible for configuration mixing. Our calculation is limited insofar as we neglect the three body component of the interaction. We also make approximations by limiting the number of intermediate states that we sum over. We include a calculation of two gluon annihilation for isoscalar mesons, a case of particular interest.

In section 6 we turn the formal results of section 5 into concrete numerical results. Intermediate numerical results are presented in such a way that they may be compared with the results of other workers. For this reason we often include accuracy in our numerical results not warranted by the approximations that we have made.

In section 7 we introduce the notation of coefficients of fractional parentage, and some explicit results. The final use to which these coefficients are put, is somewhat banal. However the notation is developed with more ambitious tasks in mind, regrettably not part of this thesis.

The results that we present for the coefficients of fractional parentage give insight into the nature of the dominant admixture for ground state nucleons. Assuming that the admixture is significant, these are essential for the calculation of some nucleon static properties such as the magnetic moment, charge radius etc.

In section 8 we show graphically some of the more immediate consequences of the results in section 6.

Finally in section 9 we make some comments on the results.

2. QUANTUM CHROMODYNAMICS

Relativistic quantum field theories, based on the principle of local gauge invariance (Ya 54), have been extremely successful in describing a large body of experimental data. The so-called gauge theories are now believed to give a complete and correct description of all non-gravitational interactions. Subsequent to the proof of renormalizability (tH 71), this class of relativistic quantum field theories has moved to the centre stage of particle physics.

Quantum Electrodynamics (QED), which describes the electromagnetic interactions of charged particles and photons, has passed tests at a high level of precision. Quantum Flavourdynamics, which describes the electroweak interactions of leptons and quarks in a unified way (We 67), successfully predicted the existence of the W and Z bosons. Finally Quantum Chromodynamics (QCD) (Fr 73) is believed to describe the strong interactions of quarks and gluons. Together these theories are known as the Standard Model of electroweak and strong interactions of quarks and leptons.

The remaining obstacles preventing whole-hearted acceptance of Quantum Chromodynamics are not primarily due to possible inconsistencies in the theory, nor to a lack of precise experimental data. The main problem lies in translating this difficult theory into concrete numerical predictions, that can be compared with experiment. Thus the possibility cannot be excluded that our present understanding of the theory is still partly incomplete and new concepts will have to be introduced.

2.1 The Motivation for Colour

Hadrons are composite objects consisting mainly of three (anti)quarks or a quark-antiquark pair (Ge 64). Initially this was thought of as merely a 'book-keeping device', but now the quarks together with the leptons, at the presently available energies,

are established as the fundamental building blocks of matter. Their interactions are described by the Standard Model (Ha 84, Cl 79).

Quantum Chromodynamics is based on the following two assumptions (Fr 73):

(a) Quarks exist in three colour states which are members of the fundamental triplet representation $\{3\}$ of the group SU(3) (de 63). By gauging this symmetry, i.e. by making the theory invariant under local gauge transformations, we arrive at a theory which describes the dynamics of the interacting quarks and gluons. Direct products of the fundamental triplet representation with itself, or with its contragredient representation $\{\bar{3}\}$ may be expressed as a linear combination of other irreducible representations,

$$\{3\} \otimes \{3\} \otimes \{3\} = \{1\} \oplus \{8\} \oplus \{8\} \oplus \{10\},$$

$$\{3\} \otimes \{\bar{3}\} = \{1\} \oplus \{8\}.$$

(b) All observed hadrons are colour singlets $\{1\}$. This means that their wavefunctions are invariant under 'rotations' in colour space. This property is consistent with the experimental observation that the colour carrying constituents of matter always seem to be confined to a finite region of space. It is generally believed that this confinement property is a consequence of QCD, but this conjecture remains to be proven.

We briefly review evidence motivating these two assumptions:

(i) The Δ^{++} consists of three spin 1/2 u quarks in a spin symmetric state. If all quarks are in the ground state, the orbital wavefunction will be symmetric in the orbital labels, which makes the overall wavefunction symmetric. However quarks are fermions and we expect the overall wavefunction to be antisymmetric. In order to preserve the

Pauli principle at least three additional degrees of freedom must be present.

(ii) The experimental cross section for e^+e^- annihilation into hadrons is larger by a factor of three than expected for uncoloured quarks. This motivates the existence of exactly three additional degrees of freedom.

(iii) The rate of decay of the neutral pi-meson into two photons is sensitive to the number of colours. The results support the three colour picture.

(iv) Assumption (b) is consistent with the absence of hadrons composed of two or four quarks. However it does not explain the absence of colour neutral exotic states like $q^2\bar{q}^2$, $q^4\bar{q}$ or gg.

All these arguments motivate the existence of the hidden colour degree of freedom in hadrons. It is important, however, to note that the concept of colour is, at the same time, the basis for the dynamics of the interacting quarks and gluons.

In the late sixties, results from deep inelastic scattering of electrons on nucleons gave a picture of nearly free pointlike constituents of nucleons. Gradually it became clear that these 'partons' were the quarks.

In 1973 it was shown (Gr 73, Po 73) that unbroken non-Abelian theories with not too many flavours of fermions were asymptotically free. For these theories the effective or running coupling constant becomes very small at high momentum transfers. This provides a natural explanation for the fact that the quarks behave as nearly free particles in the deep inelastic scattering experiments. It also provides some justification for the use of perturbation theory at high momentum transfers.

The infra-red behaviour of QCD is, however, still not understood, although it seems plausible that confinement may emerge from the theory.

2.2 Chromodynamics

We now review the classical gauge theory. The Lagrangian for a free massive fermion is given by

$$\mathcal{L} = \bar{\psi} (i \gamma_\mu \partial^\mu - M) \psi . \tag{2.1}$$

In addition to the Dirac indices implicit above, ψ carries a colour index c=1,2,3. The mass matrix is diagonal and depends only on flavour. We may apply a local gauge transformation to

$$\psi'_{c'} (x) = U_{c'c} (x) \psi_c (x) . \tag{2.2}$$

Here we use Einstein's summation convention. U(x) is given by

$$U_{c'c} (x) = exp \{ -i (\vec{\lambda}/2)_{c'c} \cdot \vec{\omega} (x) \} . \tag{2.3}$$

For each space-time point U may be a different element of the group SU(3), i.e. a complex 3x3 matrix with $U^+ = U^{-1}$ and det U=1. Eq (2.3) is the most general form of such a transformation, where the eight independent real functions ω_a are arbitrary. The $\lambda^a/2$ are the eight generators of SU(3), and the λ^a are the Gell-Mann matrices. The scalar product in colour space is defined as

$$\vec{A} \cdot \vec{B} = \sum_{a=1}^{8} A_a B_a . \tag{2.4}$$

The index a runs over the eight colour degrees of freedom of the gluon, which corresponds to the adjoint or regular representation of SU(3). The generators and their commutation relations define the Lie algebra and structure constants of SU(3),

$$[\lambda^a/2 , \lambda^b/2] = i f_{abc} \lambda^c/2 . \tag{2.5}$$

The structure constants of the group can be used to define the vector product in colour space,

$$(\vec{A} \times \vec{B})_a = \sum_{b,c=1}^{8} f_{abc} A_b B_c . \qquad (2.6)$$

The mass term of the Lagrangean (2.1) is invariant under the transformation (2.2), but the derivative term is not. To restore gauge invariance we must replace the ordinary derivative by the covariant derivative

$$D_\mu = \partial_\mu - i g \, \vec{\lambda}/2 \cdot \vec{A}_\mu(x) . \qquad (2.7)$$

Local gauge invariance of the Lagrangean will be ensured if the covariant derivative transforms as

$$D'_\mu \psi' = U (D_\mu \psi) . \qquad (2.8)$$

This can be solved to give the transformation properties of the gluon field,

$$\vec{\lambda}/2 \cdot \vec{A}'_\mu = U \vec{\lambda}/2 \cdot A_\mu U^{-1} - i/g \, (\partial_\mu U) U^{-1} . \qquad (2.9)$$

For an infinitesimal transformation $\varepsilon \omega(x)$ this gives

$$\vec{A}'_\mu(x) = \vec{A}_\mu(x) - \varepsilon/g \, \partial_\mu \vec{\omega}(x) + \varepsilon \, \vec{\omega}(x) \times \vec{A}_\mu(x) \qquad (2.10)$$

The Lagrangean now describes quarks that couple to the gluon gauge field. We need an additional kinetic term in the Lagrangean for the gluons. In QED the photon kinetic term is

$$\mathcal{L} = -1/4 \, F_{\mu\nu} F^{\mu\nu} , \qquad (2.11)$$

where the field tensor $F_{\mu\nu}$ is linearly related to the vector field A_ν,

$$F_{\mu\nu} = \partial_\mu A_\nu - \partial_\nu A_\mu . \qquad (2.12)$$

A naive generalization to the non-Abelian case suggests

$$\mathcal{L}' = -1/4\ \vec{F}_{\mu\nu} \cdot \vec{F}^{\mu\nu}, \tag{2.13}$$

where the field strength is defined by

$$\vec{F}_{\mu\nu} = \partial_\mu \vec{A}_\nu - \partial_\nu \vec{A}_\mu . \tag{2.14}$$

However this $\mathcal{L}'$ is globally, but not locally gauge invariant. The correct relation between the field strength $\vec{F}_{\mu\nu}$ and the vector field $\vec{A}_\mu$ can be found by considering the commutator of the covariant derivatives, the Bianchi identity,

$$[\ D^\mu,\ D^\nu\ ] = -ig\ \vec{\lambda}/2 \cdot \vec{F}^{\mu\nu}. \tag{2.15}$$

From this we see that

$$\vec{F}^{\mu\nu} = \partial^\mu \vec{A}^\nu - \partial^\nu \vec{A}^\mu + g\ \vec{A}^\mu \times \vec{A}^\nu . \tag{2.16}$$

The non-linear term makes the $\mathcal{L}'$ of (2.13) locally gauge invariant. Finally we may write the QCD Lagrangean as

$$\mathcal{L}_{QCD} = \bar{\psi}(i\partial_\mu D^\mu - M)\psi - 1/4\ \vec{F}_{\mu\nu} \cdot \vec{F}^{\mu\nu}. \tag{2.17}$$

2.3 Quantization

We would like to quantize the fields apearing in the QCD Lagrangean. Unfortunately the canonical conjugate momentum $\vec{\pi}^0$ of $\vec{A}^0$ vanishes. This poses a problem in both canonical and path integral formulations of quantum field theories. The problem is related to the gauge freedom, and in order to proceed we choose a specific gauge. The Coulomb gauge has been used for bag model calculations (Le 79), but has the disadvantage of not being manifestly covariant.

The resolution of the difficulties involved in canonical quantization is discussed in general in (Ku 79) and in a convenient and

lucid form for QCD in (Bu 83, Zi 86, Bu 86). We base our treatment on the latter. The result is a well defined and consistent theory which has been shown to be renormalizable (Be 74, Be 76).

Our intention is to calculate certain processes in perturbation theory for which we will need only the quark-quark-gluon vertex. For this reason we simply sketch the outline of the quantization procedure in order to provide the background and notation for our specific calculations.

The standard approach is to add a globally gauge invariant and covariant gauge fixing term

$$\mathcal{L}_{fix} = -\lambda/2 \; (\partial_\mu \vec{A}^\mu) \cdot (\partial_\nu \vec{A}^\nu) \tag{2.18}$$

where λ is a real gauge fixing parameter.

This additional gauge fixing term breaks the local gauge invariance. However, if the phases ω satisfy the constraint

$$\partial_\mu \mathcal{D}^\mu \vec{\omega} = 0 \,, \tag{2.19}$$

where $\mathcal{D}^\mu$ is given by

$$\mathcal{D}_\mu \vec{\omega} = \partial_\mu \vec{\omega} + g \, \vec{A}_\mu \times \vec{\omega} \,, \tag{2.20}$$

then we can restore some kind of gauge invariance. The constraint (2.19) is realized with the method of Lagrange multipliers by the addition of the so-called Fadeev-Popov (Fa 67) ghost term,

$$\mathcal{L}_{ghost} = i \, \vec{\chi} \cdot \partial_\mu \mathcal{D}^\mu \vec{\omega} \,, \tag{2.21}$$

and the Lagrangean density becomes

$$\mathcal{L} = \mathcal{L}_{QCD} + \mathcal{L}_{fix} + \mathcal{L}_{ghost} \tag{2.22}$$

The Lagrangean now has a new type of global gauge invariance, the Becchi-Rouet-Stora (BRS) invariance, which is sufficient to guarantee renormalizibility (Be 74, Be 76). For the explicit BRS transformations and conserved currents in our notation see (Zi 86).

The canonical conjugate momenta for the quarks, gluons and ghosts are

$$\pi = \partial\mathcal{L}/\partial\dot{\psi} = i/2\,\psi^{+}, \tag{2.23}$$

$$\bar{\pi} = \partial\mathcal{L}/\partial\dot{\bar{\psi}} = -i/2\,\bar{\psi}^{+}, \tag{2.24}$$

$$\vec{\Pi}^{k} = \partial\mathcal{L}/\partial\dot{\vec{A}}_{k} = \vec{F}^{k0}, \tag{2.25}$$

$$\vec{\Pi}^{0} = \partial\mathcal{L}/\partial\dot{\vec{A}}_{\cdot} = -\lambda\,\partial_{\mu}\vec{A}^{\mu}, \tag{2.26}$$

$$\vec{\chi} = \partial\mathcal{L}/\partial\dot{\vec{\chi}} = -i\,\mathcal{D}_{0}\,\vec{\omega}, \tag{2.27}$$

$$\vec{\Omega} = \partial\mathcal{L}/\partial\dot{\vec{\omega}} = i\,\dot{\vec{\chi}}. \tag{2.28}$$

The Hamiltonian density will now be given by

$$\mathcal{H} = -\pi\dot{\psi} + \dot{\bar{\psi}}\bar{\pi} + \vec{\Pi}_{\mu}\cdot\dot{\vec{A}}^{\mu} + \dot{\vec{\chi}}\cdot\vec{\chi} + \dot{\vec{\omega}}\cdot\vec{\Omega} - \mathcal{L}. \tag{2.29}$$

This may be divided into a g independent term, and terms linear and quadratic in g,

$$\mathcal{H} = \mathcal{H}_{0} + \mathcal{H}_{int}. \tag{2.30}$$

Integrating over the space variables we arrive at the Hamiltonian H,

$$H = H_{0}(t) + H_{int}(t) = \int d^{3}x\,\mathcal{H}_{0}(\underset{\sim}{x},t) + \int d^{3}x\,\mathcal{H}_{int}(\underset{\sim}{x},t) \tag{2.31}$$

where the non-interacting part is given by

$$\mathcal{H}_0 = \bar{\psi}\left(-\tfrac{i}{2}\gamma_k \overleftrightarrow{\partial}^k + M\right)\psi + \tfrac{1}{4}(\partial_k \vec{A}^\ell - \partial_\ell \vec{A}^k).(\partial_k \vec{A}^\ell - \partial_\ell \vec{A}^k)$$
$$+ \tfrac{1}{2}\vec{\pi}^k.\vec{\pi}^k - \tfrac{1}{2\lambda}\vec{\pi}^0.\vec{\pi}^0 + \vec{\pi}^k.\partial_k \vec{A}^0$$
$$- \vec{\pi}^0.\partial_k \vec{A}^k - i\vec{\Omega}.\vec{\chi} - i\partial_k \vec{\chi}.\partial_k \vec{\omega}, \qquad (2.32)$$

and the interaction term is

$$\mathcal{H}_{int} = -g\bar{\psi}\gamma_\mu \tfrac{\vec{\lambda}}{2}\psi.\vec{A}^\mu - \tfrac{1}{2}g(\partial_k \vec{A}^\ell - \partial_\ell \vec{A}^k).(\vec{A}^k \times \vec{A}^\ell)$$
$$- g\vec{\pi}^k.(\vec{A}^k \times \vec{A}^0) + \tfrac{1}{4}g^2(\vec{A}^k \times \vec{A}^\ell).(\vec{A}^k \times \vec{A}^\ell)$$
$$+ g\vec{\Omega}.(\vec{A}^0 \times \vec{\omega}) + ig\partial_k \vec{\chi}.(\vec{A}^k \times \vec{\omega}) \qquad (2.33)$$

Due to couplings involving time derivatives $\mathcal{H}_{int}$ is not the same as $-\mathcal{L}_{int}$.

The full Hamiltonian contains the vertices shown in Fig 2.1.

(a) (b) (c) (d)

Figure 2.1 The four vertices of BRS invariant QCD: (a) quark-quark-gluon; (b) ghost-ghost-gluon; (c) three gluon; (d) four gluon.

We quantize the fields by imposing the equal time (anti)commutation relations on the quark, gluon and ghost fields,

$$\{ \psi_{cf\alpha}(\underset{\sim}{x},t) , \psi^{\dagger}_{c'f'\alpha'}(\underset{\sim}{y},t) \} = \delta_{cc'} \delta_{ff'} \delta_{\alpha\alpha'} \delta(\underset{\sim}{x}-\underset{\sim}{y}) , \tag{2.34}$$

$$[A^{\mu}_{a}(\underset{\sim}{x},t) , \pi^{\nu}_{b}(\underset{\sim}{y},t)] = i g^{\mu\nu} \delta_{ab} \delta(\underset{\sim}{x}-\underset{\sim}{y}) , \tag{2.35}$$

$$\{ \omega_a(\underset{\sim}{x},t), \Omega_b(\underset{\sim}{y},t) \} = -i \delta_{ab} \delta(\underset{\sim}{x}-\underset{\sim}{y}) , \tag{2.36}$$

$$\{ \chi_a(\underset{\sim}{x},t), X_b(\underset{\sim}{y},t) \} = -i \delta_{ab} \delta(\underset{\sim}{x}-\underset{\sim}{y}) . \tag{2.37}$$

After quantization the quark, gluon and ghost fields become field operators in the Heisenberg picture. In the Heisenberg picture a general field operator F(x,t) will satisfy the Heisenberg equation of motion,

$$i \, \partial/\partial t \; F(\underset{\sim}{x},t) = [F(\underset{\sim}{x},t) , H] \tag{2.38}$$

Thus, in order to covariantly quantize, we have expanded our Hilbert space to include a quartet of unphysical fields. The scalar and longitudinally polarized gluons, and the two spin zero fermionic ghosts.

Associated with these unphysical fields are state vectors which have negative norm i.e. our Hilbert space has an indefinite metric. In order to retain the probabilistic interpretation of the theory it is necessary to find a subspace of the full Hilbert space which describes physical states. In QED the Gupta-Bleuler subsidiary condition (Gu 50, Bl 50) discriminates between physical and unphysical states :

$$\partial_{\mu} A^{\mu (+)} \; | \psi_{phys} > = 0 \tag{2.39}$$

Here the plus sign denotes the positive frequency part of the field operator.

An analogous operator, based on the BRS charge, exists in the non-Abelian case, with the added complication that it has a g-dependent part. However, for asymptotic states it is sufficient that the Gupta-Bleuler condition, and a similar condition for the ghosts hold. Physical states may always be chosen such that they do not contain scalar and longitudinal gluons and ghosts.

3. PERTURBATION THEORY

Unfortunately, it has not yet been possible to find exact solutions to QCD, and we therefore have to rely on perturbation theory, or other approximative schemes. However, it likely that the confinement mechanism can only be understood by non-perturbative methods. The hope is that for some of the processes internal to baryons, a perturbative description may be adequate. Also, the matrix elements obtained from the perturbation theory may be plugged into a description based on diagonalization of a truncated space, as in the treatment of (Ba 84). Truncated spaces including gluons in the basis will require a correct treatment of the self energy.

3.1 The Gell-Mann and Low Theorem

After quantization the operators and state vectors of the quantum field theory are given in the Heisenberg picture. In doing perturbation theory it is useful to transform into the interaction or Dirac picture. We denote interaction picture operators and state vectors by a hat. The unitary transformation from Heisenberg state vectors to interaction picture state vectors is given by

$$|\hat{\Psi}(t)\rangle = U(t)\,|\Psi\rangle, \tag{3.1}$$

where U(t) satisfies the differential equation

$$i\,\frac{\partial}{\partial t}\,U(t) = U(t)\,H_{int}(t). \tag{3.2}$$

Similarly, a general Heisenberg operator F(x,t) is transformed into a Dirac operator by

$$\hat{F}(\underset{\sim}{x},t)=U(t)\ F(\underset{\sim}{x},t)\ U^{-1}(t)\ . \tag{3.3}$$

Under this transformation all operator equations written in terms of the fields, their canonical momenta, and spatial derivatives thereof, remain formally the same. For example, the canonical commutation relations remain unchanged.

The Heisenberg equation of motion in the case of Dirac operators is given by

$$i\ \frac{\partial}{\partial t}\ \hat{F}(\underset{\sim}{x},t) = \left[\ \hat{F}(\underset{\sim}{x},t)\ ,\hat{H}_o\right]. \tag{3.4}$$

Thus, expressions involving time derivatives of field operators do not remain formally identical as we transform from the Heisenberg to the Dirac picture. The Hamiltonian expressed in terms of the fields, canonical momenta and spatial derivatives is formally unchanged. However this is not so when it is expressed in terms of the fields and their 4-derivatives.

The Schrodinger equation of motion for a state vector in the Dirac picture is given by

$$i\ \frac{\partial}{\partial t}\ |\hat{\Psi}(t)> = \hat{H}_{int}(t)\ |\hat{\Psi}(t)>. \tag{3.5}$$

If we define

$$U(t,t_o) = U(t)\,U^{-1}(t_o), \tag{3.6}$$

then the time evolution of a Dirac state vector is

$$|\hat{\Psi}(t)> = U(t,t_o)\ |\hat{\Psi}(t_o)>\ . \tag{3.7}$$

From Equations (3.2), (3.3) and (3.6) we can show

$$i \frac{\partial}{\partial t} U(t,t_0) = \hat{H}_{int}(t)\, U(t,t_0), \tag{3.8}$$

and clearly

$$U(t_0,t_0) = \mathbb{1}. \tag{3.9}$$

By integrating (3.8) subject to (3.9) we arrive at Dysons expansion for the time evolution operator

$$U(t,t_0) = \sum_{n=0}^{\infty} \frac{(-i)^n}{n!} \int_{t_0}^{t} dt_1 .. dt_n\, T\left[\hat{H}_{int}(t_1) .. H_{int}(t_n)\right] \tag{3.10}$$

where T denotes the time ordering operator. We now introduce a damping factor such that for $t \to \pm\infty$ our Hamiltonian $\hat{H}$ tends to the non-interacting Hamiltonian $\hat{H}_0$. At the same time we introduce a parameter λ that will be set to 1 at the end of the calculation,

$$\hat{H}(t) = \hat{H}_0 + e^{-\varepsilon|t|} \lambda\, \hat{H}_{int}(t) \tag{3.11}$$

The parameter λ enables us to talk of powers in the interaction strength, and it should not be confused with g, as some terms of the Hamiltonian are of order g^2. At the end of the calculation we will let $\varepsilon > 0$ tend to zero. The new time evolution operator $U_\varepsilon(t,t_0)$ is given by (3.10) where $\hat{H}_{int}(t)$ is replaced by the second part of (3.11). We now assume that there exists an exact eigenstate $|\hat{\phi}\rangle$ of $\hat{H}_0$,

$$\hat{H}_0 |\hat{\phi}\rangle = E_0 |\hat{\phi}\rangle \tag{3.12}$$

In the limit $t \to \pm\infty$, this time independent interaction picture state vector is an eigenstate of the Hamiltonian (3.11). One might therefore hope that the state

$$|\hat{\Psi}(0)\rangle = U_\varepsilon(0,-\infty)\, |\hat{\phi}\rangle \tag{3.13}$$

is, in the limit $\varepsilon \to 0^+$, the exact eigenstate of $\hat{H}(0)$. This limit does not exist, because the expression contains a divergent phase. However, the Gell-Mann and Low theorem (Ge 51, Fe 71) guarantees that, if

$$|\hat{\psi}\rangle = \lim_{\varepsilon \to 0^+} \frac{U_\varepsilon(0,-\infty)|\hat{\phi}\rangle}{\langle\hat{\phi}|U_\varepsilon(0,-\infty)|\hat{\phi}\rangle} \tag{3.14}$$

exists to all powers of λ, then it is an exact eigenstate of $\hat{H}(0)$, with the eigenvalue E. Clearly not all systems will satisfy this condition and even if they do, the eigenstates thus generated may not include all eigenstates of $\hat{H}$. We should note at this point that our perturbation series will exhibit divergences which are related to the ultraviolet singularities in Quantum Field Theory. However these divergences do not affect the validity of the Gell-Mann and Low theorem as they may in principle be removed by appropriate counterterms in the Lagrangean. This is a consequence of the fact that QCD is renormalizable.

The energy shift is given by

$$\Delta E = E - E_0 = \lim_{\varepsilon \to 0^+} \frac{\langle\hat{\phi}|\lambda \hat{H}_{int}(0) U_\varepsilon(0,-\infty)|\hat{\phi}\rangle}{\langle\hat{\phi}|U_\varepsilon(0,-\infty)|\hat{\phi}\rangle} \tag{3.15}$$

Thus far we have not specified whether $|\hat{\phi}\rangle$ is a ground state or an excited state, or whether it is degenerate or non-degenerate.

3.2 Degenerate States

In using the Gell-Mann and Low theorem we should take a little extra care when dealing with degenerate states. The theorem, in its original form, does not refer to possible degeneracy of the initial unperturbed state. The initial state may be chosen as an arbitrary linear combination of degenerate states. The essential point is that for degenerate states, if the degeneracy is lifted in some order of λ, then some coefficient of λ will diverge. The Gell-Mann and Low eigenvector only exists for special linear combinations of the unperturbed states. These states are the states to which the exact eigenstates of the full Hamiltonian tend as $\lambda \to 0$.

In order to demonstrate this problem we examine a simple case, a doubly degenerate eigenstate of $\hat{H}_0$, $|\phi_i\rangle$, i=1,2 in which the degeneracy is lifted in lowest order. The energy shift as a power series in λ is given by

$$\Delta E = \lim_{\varepsilon \to 0^+} \frac{\langle \hat{\phi}_i | \lambda \hat{H}_{int}(0)\, U_\varepsilon(0,-\infty) | \phi_i \rangle}{\langle \hat{\phi}_i | U_\varepsilon(0,-\infty) | \hat{\phi}_i \rangle} \tag{3.16}$$

$$= \lim_{\varepsilon \to 0^+} \lambda \langle \hat{\phi}_i | \hat{H}_{int}(0) | \hat{\phi}_i \rangle + \lambda^2 (-i) \int_{-\infty}^{0} dt\, e^{-\varepsilon |t|}$$

$$\times \left\{ \langle \hat{\phi}_i | \hat{H}_{int}(0) \hat{H}_{int}(t) | \hat{\phi}_i \rangle - \langle \hat{\phi}_i | \hat{H}_{int}(0) | \hat{\phi}_i \rangle \langle \hat{\phi}_i | \hat{H}_{int}(t) | \phi_i \rangle \right\} + O(\lambda^3) \tag{3.17}$$

The time dependence of the interaction picture operator $\hat{H}_{int}(t)$ can be made explicit by use of the Heisenberg equation of motion (3.4),

$$\hat{H}_{int}(t) = e^{i\hat{H}_0 t}\, \hat{H}_{int}(0)\, e^{-i\hat{H}_0 t} . \tag{3.18}$$

We now simplify equation (3.17) by inserting a complete set of states in the second term and performing the time integration. We get

$$\Delta E = \lambda \langle \hat{\phi}_i | \hat{H}_{int}(0) | \hat{\phi}_i \rangle$$

$$+ \sum_{n \neq i} \lambda^2 \frac{-1}{E_n - E_i} \langle \hat{\phi}_i | \hat{H}_{int}(0) | \hat{\phi}_n \rangle \langle \hat{\phi}_n | \hat{H}_{int}(0) | \hat{\phi}_i \rangle + O(\lambda^3) \qquad (3.19)$$

Thus the $O(\lambda^2)$ term diverges due to the energy denominator unless $\hat{H}_{int}(0)$ is diagonal in the degenerate subspace.

In summary, we can use the Gell-Mann and Low theorem for degenerate states as well. Firstly we must diagonalize the degenerate subspace in the lowest order of λ in which the degeneracy is lifted. These new states become the starting point for higher order calculations.

3.3 Goldstone's Theorem

We now wish to evaluate the matrix elements of the time ordered products in (3.15). Using Wick's theorem we may decompose the time ordered product into a sum of normal ordered products consisting of all possible contracted and uncontracted permutations of the operators. If $|\hat{\phi}\rangle$ is the vacuum the expectation values of uncontracted operators will vanish due to the normal ordering.

The usual path would now be to use Goldstone's theorem (Go 57). We assume a thorough familiarity with the treatment of (Fe 71). The denominator of (3.15) cancels leaving only 'connected' diagrams in the numerator. By 'connected' we mean contracted indirectly or directly to $\hat{H}_{int}(0)$. This gives

$$\Delta E = \lim_{\varepsilon \to 0+} \langle \hat{\phi} | \hat{H}_{int}(0)\, U_\varepsilon(0, -\infty) | \hat{\phi} \rangle_{connected} \qquad (3.20)$$

We may not use this theorem, as is sometimes implicitly assumed (Cl 80), because we wish to perturb states $|\hat{\phi}\rangle$, other than the vacuum. In order to clarify the issue we consider a two quark system,

$$|\hat{\phi}\rangle = a_1^\dagger a_2^\dagger |\hat{0}\rangle \tag{3.21}$$

$|\hat{\phi}\rangle$ is an interaction picture state vector for $t \to -\infty$, and is, as previously discussed time independent. The quark creation operators above are time independent, i.e. not in the interaction picture, but in the Schrodinger picture. This may seem to be an apparent paradox, but some thought will convince one that this is correct. Equation (3.15) now becomes

$$\Delta E = \lim_{\varepsilon \to 0^+} \frac{\langle \hat{0} | a_2 a_1 \hat{H}_{int}(0) U_\varepsilon(0,-\infty) a_1^\dagger a_2^\dagger | \hat{0} \rangle}{\langle \hat{0} | a_2 a_1 U_\varepsilon(0,-\infty) a_1^\dagger a_2^\dagger | \hat{0} \rangle} \tag{3.22}$$

We wish to perform a Wick decomposition in which matrix elements of all terms containing uncontracted operators vanish. We would therefore like all operators inside the time ordered product. We attach <u>dummy</u> time arguments to the quark creation and annihilation operators and bring them into the time ordered product,

$$\begin{aligned} a_1^\dagger a_2^\dagger &\to a_1^\dagger(-\infty)\ a_2^\dagger(-\infty) \\ a_1\ a_2 &\to a_1(0)\ a_2(0) \end{aligned} \tag{3.23}$$

When contractions involving these operators are evaluated it should be taken into account that they are not interaction picture operators. The numerator will now consist of terms like :

$$\langle \hat{0} | T\left[a_2(0) a_1(0) \hat{H}_{int}(0) \hat{H}_{int}(t_1) \cdots \hat{H}_{int}(t_n) a_1^\dagger(-\infty) a_2^\dagger(-\infty)\right] | \hat{0} \rangle \tag{3.24}$$

The Wick decomposition of this is a sum of terms. Each term is a normal ordered product of all operators in the time ordered product, with some contracted. Since we will evaluate the expectation value with respect to the vacuum, we need only consider those terms in which all operators are contracted with some other operator.

Each matrix element may be represented by a Feynman diagram. The operators may be grouped into sets, such that each operator is 'connected' to every other operator in the set via the propagators and vertices of the part of the diagram representing the set. This part of the diagram will not be connected to the rest of the diagram. The matrix element of each such set is a c number, so we may factorize each term into a product of such sets.

Any two operators in a given set we refer to as 'connected' to each other. Operators in different sets are 'disconnected' from each other. For example, in equation (3.20) all operators must be connected to $\hat{H}_{int}(0)$.

We refer to the operators of (3.23) as external operators. Our primary interest is in the connection properties of the operators that make up the expansion of the time evolution operator, namely the $\hat{H}_{int}(t_i)$'s. In Fig 3.1 we show some possible diagrams and introduce some terminology, as well as abbreviations, describing terms in the expansion.

Fig 3.1 : (a) 'totally disconnected'='tot disc'; (b) 'connected to $\hat{H}_{int}(0)$'='H conn', (c) 'externally connected'='ext conn', (d) 'externally connected and connected to $\hat{H}_{int}(0)$'

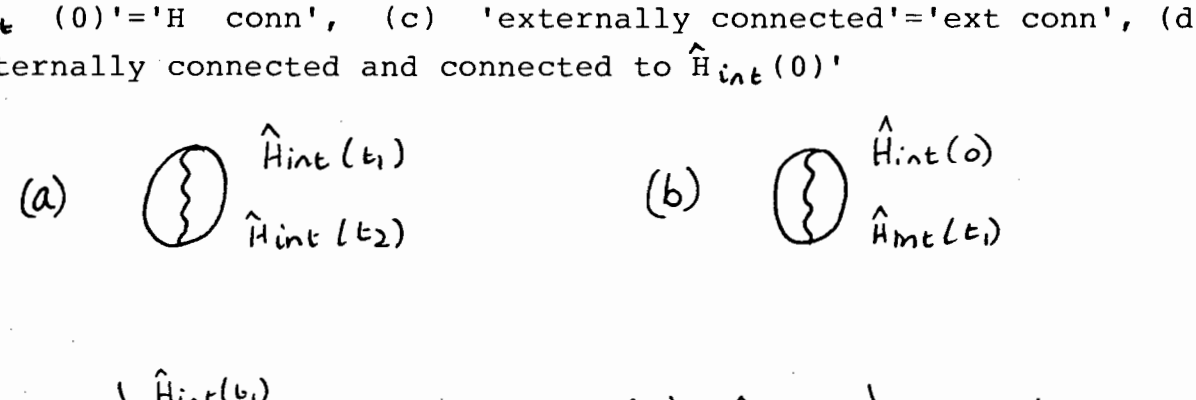

In order to implement an adapted form of Goldstone's theorem, we consider the following expression,

$$\sum_{n=0}^{\infty} \frac{(-i)^n}{n!} \int_{-\infty}^{0} dt_1 \ldots dt_n \langle 0 | T[A(0)B(0)\hat{H}_{int}(t_1) \ldots H_{int}(t_n)] | 0 \rangle \quad (3.25)$$

We suppose that there are m $\hat{H}_{int}(t)$'s that are A and/or B connected and p remaining $\hat{H}_{int}(t)$'s that are totally disconnected. Clearly n=m+p. This partition can be done in n!/m!p! ways. (3.20) becomes

$$\sum_m \sum_p (-i)^{m+p} \frac{n!}{m!p!} \frac{1}{n!} \int_{-\infty}^{\infty} dt_1 .. dt_m \int_{-\infty}^{\infty} dt'_1 .. dt_p$$
$$\langle 0 | T[A(0) B(0) \hat{H}_{int}(t_1) .. \hat{H}_{int}(t_m)] | 0 \rangle_{A \text{ and/or } B \text{ conn}}$$
$$\langle 0 | T[\hat{H}_{int}(t'_1) .. \hat{H}_{int}(t'_p)] | 0 \rangle \qquad (3.26)$$

By 'A and/or B conn' we mean that each $H_{int}(t)$ is connected to either A or B or both. This does not imply that each $H_{int}(t)$ is connected to every other $H_{int}(t)$. Condensing the notation we have shown

$$\langle A(0) B(0) U_\varepsilon(0,-\infty) \rangle = \langle A(0) B(0) U_\varepsilon(0,-\infty) \rangle_{\substack{A \text{ and/or } B \\ conn}} \langle U_\varepsilon(0,-\infty) \rangle \qquad (3.27)$$

We can immediately apply this factorization procedure to (3.24) and cancel all totally disconnected diagrams from its numerator and denominator. Now all the terms in the numerator will be 'externally and/or $H_{int}(0)$ connected' and all the terms in the denominator will be 'externally connected'. (3.15) becomes, with obvious abbreviations

$$\Delta E = \lim_{\varepsilon \to 0^+} \frac{\langle 0 | a_2 a_1 \hat{H}_{int}(0) U_\varepsilon(0,-\infty) a_1^\dagger a_2^\dagger | 0 \rangle_{ext \text{ and/or } H \text{ conn}}}{\langle 0 | a_2 a_1 U_\varepsilon(0,-\infty) a_1^\dagger a_2^\dagger | 0 \rangle_{ext \text{ conn}}} \qquad (3.28)$$

The numerator contains terms in which $H_{int}(0)$ is directly or indirectly connected to at least one external line (such as Fig 3.1 (d.)), and terms where this is not the case (such as a product of Fig 3.1 (b.) and (c.)). We denote the former '$H_{int}(0)$-external connected. We split the numerator into a sum of each type. The '$H_{int}(0)$-external disconnected' sum may be factorized, giving

$$\langle 0|\, a_2 a_1\, \hat{H}_{int}(0)\, U_\varepsilon(0,\infty)\, a_1^\dagger a_2^\dagger\, |0\rangle_{ext \text{ and/or } H \text{ conn}}$$

$$= \langle 0|\, a_2 a_1\, \hat{H}_{int}(0)\, U_\varepsilon(0,-\infty)\, a_1^\dagger a_2^\dagger |0\rangle_{H\text{-}ext \text{ conn}}$$

$$+ \left\{ \langle 0|\, a_2 a_1\, U_\varepsilon(0,-\infty)\, a_1^\dagger a_2^\dagger\, |0\rangle_{ext \text{ conn}} \langle 0|\, H_{int}(0)\, U_\varepsilon(0,-\infty)|0\rangle_{H \text{ conn}} \right\} \quad (3.29)$$

One of the terms corresponds precisely with the denominator, cancelling it leaves

$$\Delta E = \Delta E_{part} + \Delta E_{vacuum} \quad (3.30)$$

where

$$\Delta E_{vacuum} = \langle 0|\, H_{int}(0)\, U_\varepsilon(0,-\infty)|0\rangle_{H \text{ conn}}$$

$$\Delta E_{part} = \frac{\langle 0|\, a_2 a_1\, H_{int}(0)\, U_\varepsilon(0,-\infty)\, a_1^\dagger a_2^\dagger |0\rangle_{H\text{-}ext \text{ conn}}}{\langle 0|\, a_2 a_1\, U_\varepsilon(0,-\infty)\, a_1^\dagger a_2^\dagger\, |0\rangle_{ext \text{ conn}}} \quad (3.31)$$

The need for this denominator will be clear later. We see that the total energy shift is due to the shift in energy of the vacuum taken alone, plus the energy due to the particles inserted asymptotically.

4 CAVITY QUANTUM CHROMODYNAMICS

4.1 Boundary Conditions

Experimentally it is observed that the colour carrying constituents of the hadrons are confined in a finite region of space. This confinement is probably due to the different properties of the vacua inside and outside the hadron. It is unlikely that this problem will be understood perturbatively.

In the absence of a solution to the confinement problem, we put in this experimental fact by imposing boundary conditions. These are imposed on the field operators at the surface of a cavity with volume V, in which the colour carrying constituents are confined.

While this may seem to be implicit acceptance of the MIT bag model we emphasize that this is simply the study of field theory in a finite volume. (Ba 84) has shown that this framework may be used to simulate potential models of massive quarks.

In order to delineate the volume that we wish to study, we define the step function

$$\theta(x) = \begin{cases} 1 & x \in V \\ 0 & x \notin V \end{cases} \qquad (4.1)$$

The surface delta function $\delta(x)$ is related to the step function by

$$\partial_\mu \theta(x) = n_\mu \delta(x) \qquad (4.2)$$

$\underset{\sim}{n}$ is a vector normal to the surface, pointing outwards from V, and $n_\mu = (n_0, -\underset{\sim}{n})$ is normalized to

$$n_\mu n^\mu = -1 \qquad (4.3)$$

The MIT group (Ch 74, De 75) introduced boundary conditions on the constituent field operators at the surface S,

$$(i n_\mu \gamma^\mu - 1)\psi|_S = 0 = \bar{\psi}(i n_\mu \gamma^\mu + 1)|_S \tag{4.4}$$

$$n_\mu \vec{F}^{\mu\nu}|_S = n_\mu \vec{A}^\mu|_S = n_\mu \partial^\mu (\partial_\nu \vec{A}^\nu)|_S = 0 \tag{4.5}$$

$$n_\mu \partial^\mu \vec{\omega}|_S = n_\mu \partial^\mu \vec{\chi}|_S = 0 \tag{4.6}$$

These boundary conditions are consistent with the BRS symmetry of the theory and guarantee that no quarks, gluons, or ghosts can escape the cavity. For simplicity, we restrict ourselves to a static and spherically symmetric cavity.

4.2 Quark Cavity Modes

We must now solve for the quark wavefunction in a static spherical cavity, subject to the boundary conditions (4.4). The time independent Dirac equation derived from the Lagrangean is, for the non-interacting case, g=0,

$$(-i \underset{\sim}{\gamma} \cdot \underset{\sim}{\nabla} + m_f)\, u_n(\underset{\sim}{r}) = \varepsilon_n \gamma^0 u_n(\underset{\sim}{r}) \tag{4.7}$$

where m_f is the flavour dependent mass, and ε_n the energy of cavity mode n. n stands for the flavour, radial and Dirac quantum numbers and where relevant the magnetic quantum number as well,

$$n = \{f, \nu, k, (\mu)\} \tag{4.8}$$

The wave function is given by

$$u_n(\underset{\sim}{r}) = \begin{bmatrix} g_n(r)\, \chi^\mu_k(\hat{r}) \\ i f_n(r)\, \chi^\mu_{-k}(\hat{r}) \end{bmatrix} \tag{4.9}$$

The adjoint spinor is defined by

$$\bar{u}_n(\underset{\sim}{r}) = u_n^\dagger(\underset{\sim}{r})\, \gamma^0 \tag{4.10}$$

The $\chi^{\mu}_{\kappa}(r)$ are the two-component spherical spinors. The radial functions f_n, g_n are

$$g_n(r) = \mathcal{N}_n \, R^{-3/2} \, j_\ell(p_n r),$$
$$f_n(r) = \mathcal{N}_n \, R^{-3/2} \, \mathrm{sgn}\,\kappa \, \frac{p_n}{\varepsilon_n + m_f} \, j_{\bar{\ell}}(p_n r), \qquad (4.11)$$

where the angular momentum quantum numbers are defined by

$$j(\kappa) = |\kappa| - 1/2,$$
$$\ell(\kappa) = j(\kappa) + 1/2 \, \mathrm{sgn}\,\kappa,$$
$$\bar{\ell}(\kappa) = j(\kappa) - 1/2 \, \mathrm{sgn}\,\kappa. \qquad (4.12)$$

The complete set of Dirac wavefunctions includes positive ($\nu > 0$) and negative ($\nu < 0$) energies. The eigenmodes are determined by the linear boundary condition (4.4) which simplifies to

$$j_\ell(x_n) + \frac{x_n \, \mathrm{sgn}\,\kappa}{\omega_n + \varrho_f} \, j_{\bar{\ell}}(x_n) = 0, \qquad (4.13)$$

where the dimensionless energy, momentum and mass are given by

$$\omega_n = \varepsilon_n R = \mathrm{sgn}\,\nu \, \sqrt{x_n^2 + \varrho_f^2}$$
$$x_n = p_n R$$
$$\varrho_f = m_f R \qquad (4.14)$$

The normalization constant is

$$\mathcal{N}_n^{-2} = \left[2\omega_n(\omega_n + \kappa) + \varrho_f \right] \left[\frac{j_\ell(x_n)}{x_n} \right]^2 \qquad (4.15)$$

The full set of quark eigenmodes is complete and orthonormal.

4.3 Gluon Cavity Modes

In the Feynman gauge ($\lambda=1$) we have to solve

$$(\Delta + \Omega_m^{\Sigma 2})\, a_m^{0\Sigma}(\underset{\sim}{r}) = 0 \qquad \Sigma = S \tag{4.16}$$

$$(\Delta + \Omega_m^{\Sigma 2})\, \underset{\sim}{a}_m^{\Sigma}(\underset{\sim}{r}) = 0 \qquad \Sigma = L M E \tag{4.17}$$

where Ω_m^{Σ} is the gluon eigenenergy, and the eigenmodes are given by

$$a_m^{0S}(\underset{\sim}{r}) = R^{-3/2} \mathcal{N}_m^{S}\, i\, j_J(\Omega_m^{S} r)\, Y_{JM}(\hat{r}) \qquad J \geq 0 \tag{4.18}$$

$$\underset{\sim}{a}_m^{L}(\underset{\sim}{r}) = R^{-3/2} \mathcal{N}_m^{L} \frac{1}{\Omega_m^{L}} \underset{\sim}{\nabla}\, j_J(\Omega_m^{L} r)\, Y_{JM}(\hat{r}) \qquad J \geq 0 \tag{4.19}$$

$$\underset{\sim}{a}_m^{M}(\underset{\sim}{r}) = R^{-3/2} \mathcal{N}_m^{M} \frac{L}{\sqrt{J(J+1)}} \left[j_J(\Omega_m^{M} r)\, Y_{JM}(\hat{r}) \right] \qquad J \geq 1 \tag{4.20}$$

$$\underset{\sim}{a}_m^{E}(\underset{\sim}{r}) = R^{-3/2} \mathcal{N}_m^{E}\, \underset{\sim}{\nabla} \times \frac{\underset{\sim}{L}}{\sqrt{J(J+1)}} \left[j_J(\Omega_m^{E} r)\, Y_{JM}(\hat{r}) \right] \qquad J \geq 1 \tag{4.21}$$

There are four polarizations Σ, referred to as Scalar, Longitudinal, Magnetic and Electric (S,L,M,E). m=(N,J,(M)) stands for the radial and angular momentum quantum numbers. We shall sometimes refer to a mode as NΣ J, e.g. 1M1.

The linear boundary conditions (4.5) for a static spherical cavity imply

$$\hat{r} \cdot \underset{\sim}{\nabla}\, a_m^{0S}(\underset{\sim}{r})\big|_{r=R} = 0 \tag{4.22}$$

$$\left.\begin{aligned} &\hat{r} \cdot \underset{\sim}{a}_m^{\Sigma}(\underset{\sim}{r})\big|_{r=R} = 0 && (4.23)\\ &\hat{r} \times (\underset{\sim}{\nabla} \times \underset{\sim}{a}_m^{\Sigma}(\underset{\sim}{r}))\big|_{r=R} = 0 && (4.24) \end{aligned}\right\} \Sigma = L M E$$

which simplify to

$$\frac{d}{dr} j_J(\Omega^{\Sigma}_m r)\big|_{r=R} = 0 \qquad \Sigma = s, \ell, \tag{4.25}$$

$$\frac{d}{dr} r j_J(\Omega^{\mu}_m r)\big|_{r=R} = 0, \tag{4.26}$$

$$j_J(\Omega^{\varepsilon}_m r)\big|_{r=R} = 0. \tag{4.27}$$

The normalization constants are given by

$$[\mathcal{N}^s_m]^{-2} = [\mathcal{N}^{\ell}_m]^{-2} = \tfrac{1}{2} j_J^2(y^s_m)\left[1 - \frac{J(J+1)}{(y^s_m)^2}\right], \tag{4.28}$$

$$[\mathcal{N}^{\mu}_m]^{-2} = \tfrac{1}{2} j_J^2(y^{\mu}_m)\left[1 - \frac{J(J+1)}{(y^{\mu}_m)^2}\right], \tag{4.29}$$

$$[\mathcal{N}^{\varepsilon}_m]^{-2} = \tfrac{1}{2} j_{J+1}^2(y^{\varepsilon}_m), \tag{4.30}$$

where the dimensionless energy is

$$y^{\Sigma}_m = \Omega^{\Sigma}_m R \qquad \Sigma = s, \ell, \mu, \varepsilon \tag{4.30}$$

The scalar mode is the zeroth component of a 4-vector potential so we refer to

$$a^{\mu\Sigma}_m(\underset{\sim}{r}) = \begin{cases} a^0_m(\underset{\sim}{r}) & \mu = 0\,;\ \Sigma = s \\ [\underset{\sim}{a}^{\Sigma}_m(\underset{\sim}{r})]^{\mu} & \mu = 1,2,3\,;\ \Sigma = \ell, \mu, \varepsilon \\ 0 & \text{all other } \mu, \Sigma. \end{cases} \tag{4.31}$$

Our set of cavity modes is complete,

$$\sum_{\Sigma m} g^{\Sigma\Sigma} a^{\mu\Sigma}_m(\underset{\sim}{r})^* a^{\nu\Sigma}_m(\underset{\sim}{r}') = g^{\mu\nu} \delta^3(\underset{\sim}{r}' - \underset{\sim}{r}) \tag{4.32}$$

and orthonormal,

$$\int a^{\Sigma}_{\mu m}(\underset{\sim}{r})^* a^{\mu\Sigma'}_{m'}(\underset{\sim}{r})\, d^3r = g^{\Sigma\Sigma'} \delta_{mm'} \tag{4.33}$$

Here we have introduced

$$g^{ss} = -g^{dd} = -g^{\mu\mu} = -g^{\varepsilon\varepsilon} = 1$$
$$g^{\Sigma\Sigma'} = 0 \quad \text{if} \quad \Sigma \neq \Sigma' \tag{4.34}$$

Under complex conjugation we have

$$a^{\mu\Sigma}_{m}(\underset{\sim}{r})^{*} = \eta_{\Sigma}(-)^{M} a^{\mu\Sigma}_{m^{*}}(\underset{\sim}{r}) \tag{4.35}$$

where the quantum numbers m^{*} are given by

$$m^{*} = \{N, J, (-M)\} \tag{4.36}$$

and the phase η by

$$\eta_{\Sigma} = \begin{cases} +1 & \Sigma = \mathcal{L}, \mathcal{E} \\ -1 & \Sigma = \mathcal{S}, \mathcal{M} \end{cases} \tag{4.37}$$

4.4 Cavity Mode Expansions

The field operators may be expanded in a complete and orthonormal set of functions that obey the same field equations and boundary conditions. Upon quantization, the expansion coefficients become the creation and annihilation operators for the particles and antiparticles.

The quark field operator is expressed

$$\begin{aligned} \psi_{cf}(x) &= \psi^{(+)}_{cf}(x) + \psi^{(-)}_{cf}(x) \\ &= \sum_{\kappa\mu n>0} \left[a_{cn} u_{n}(\underset{\sim}{x}) e^{-i\varepsilon_{n}t} + b^{+}_{cn} u_{-n}(\underset{\sim}{x}) e^{i\varepsilon_{n}t} \right] \\ \bar{\psi}_{cf}(x) &= \bar{\psi}^{(+)}_{cf}(x) + \bar{\psi}^{(-)}_{cf}(x) \\ &= \sum_{\kappa\mu n>0} \left[a^{+}_{cn} \bar{u}_{n}(\underset{\sim}{x}) e^{i\varepsilon_{n}t} + b_{cn} \bar{u}_{-n}(\underset{\sim}{x}) e^{-i\varepsilon_{n}t} \right] \end{aligned} \tag{4.38}$$

where we have used the symmetry relation

$$\varepsilon_{-n} = -\varepsilon_n \tag{4.39}$$

and

$$-n = \{ f, -\nu, -\kappa, (-\mu) \} \tag{4.40}$$

In the usual way a and b refer to quarks and antiquarks, thus restricting the expansion to positive ν.

The anticommutators follow from the canonical anticommutation relations, and the orthonormality of the cavity eigenmodes

$$\{ a_{cn}, a^{\dagger}_{c'n'} \} = \{ b_{cn}, b^{\dagger}_{c'n'} \} = \delta_{cc'} \delta_{nn'} \tag{4.41}$$

The gluon field operator may be expanded

$$\begin{aligned} A^{\mu}_{a}(x) &= A^{\mu}_{a}(x)^{(+)} + A^{\mu}_{a}(x)^{(-)} \\ &= \sum_{\substack{\Sigma J M \\ N>0}} 1/\sqrt{2\Omega^{\Sigma}_{m}} \left[c^{\Sigma}_{am} a^{\mu\Sigma}_{m}(\underset{\sim}{x}) e^{-i\Omega^{\Sigma}_{m} t} \right. \\ &\qquad \left. + c^{\Sigma\dagger}_{am} a^{\mu\Sigma}_{m}(\underset{\sim}{x})^{*} e^{i\Omega^{\Sigma}_{m} t} \right] \end{aligned} \tag{4.42}$$

The gluon creation and annihilation operators $c, c^{\dagger}$ obey

$$\left[c^{\Sigma}_{am}, c^{\Sigma' \dagger}_{a'm'} \right] = -g^{\Sigma\Sigma'} \delta_{aa'} \delta_{mm'} \tag{4.43}$$

4.5 Propagators in the Cavity

Based on the cavity expansion (4.38) we find the quark propagator to be

$$\begin{aligned} \langle 0 | \hat{\psi}_{cf\alpha}(x) \hat{\bar{\psi}}_{c'f'\alpha'}(y) | 0 \rangle &= \delta_{cc'} \delta_{ff'} \sum_{\substack{k_\mu \\ \nu>0}} e^{-i\varepsilon_n |x^0 - y^0|} \\ &\{ u_{n\alpha}(\underset{\sim}{x}) \bar{u}_{n\alpha'}(\underset{\sim}{y}) \theta(x^0 - y^0) - u_{-n\alpha}(x) \bar{u}_{-n\alpha'}(y) \theta(y^0 - x^0) \} \end{aligned} \tag{4.44}$$

with the usual step function

$$\theta(x^0) = \begin{cases} 1 & x^0 \geq 0 \\ 0 & x^0 < 0 \end{cases} \tag{4.45}$$

The gluon propagator, using (4.42), is given by

$$\langle 0 \mid \hat{A}^{\mu}_{a}(x)\, \hat{A}^{\nu}_{b}(y) \mid 0 \rangle = -\delta_{ab} \sum_{JM\Sigma N>0} \left\{ g^{\Sigma\Sigma}/2\Omega^{\Sigma}_{m}\; a^{\mu\Sigma}_{m}(\underset{\sim}{x})\, a^{\nu\Sigma}_{m}(\underset{\sim}{y})^{*}\, e^{-i\Omega^{\Sigma}_{m}|x^0-y^0|} \right\} \tag{4.46}$$

5 PERTURBED CAVITY QUANTUM CHROMODYNAMICS

In this section we formally calculate the perturbative energy shift of qqq or $q\bar{q}$ systems due to a selected subset of 4th order diagrams. We select for calculation those diagrams that correspond to repeated one gluon exchange, and therefore lead to a mixing of the unperturbed qqq or $q\bar{q}$ configuration with other qqq or $q\bar{q}$ configurations. Because of the dynamic nature of the gluon we will also have some intermediate states with gluon components.

In order to simplify the calculation we make some approximations. We omit some intermediate states. We do not attempt to calculate the perturbative energy shift due to three body forces. Finally we ignore all the other 4th order diagrams. This does not mean that we consider them to be unimportant, the intention is simply to make a start on a difficult problem.

The calculation of the 4th order diagrams is tedious, but it has many similarities with the 2nd order calculation. For this reason we do a detailed calculation of the 2nd order diagram, and simply write down the 4th order diagrams in correspondence with their graphical representations.

5.1 Second Order Diagrams

The second order diagrams involving asymptotic states containing quarks and antiquarks are shown in Fig 5.1.

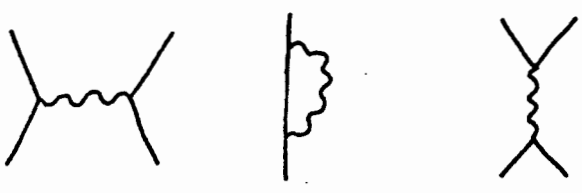

Fig 5.1 : 2nd order diagrams

The process shown in Fig 5.1(c) can only occur in the case of a quark-antiquark pair coupled to a colour octet state.

The self-energy (Fig 5.1 (b)) diverges, and after renormalization it will contribute to the single particle energy. We do not incorporate this quantity, but note that during the final preparation of this thesis a reliable calculation of this quantity was published (Go 86).

The process shown in Fig 5.1 (a) is the hyperfine or one gluon exchange process. It may also be visualized as the mixing of qq and qqg states via the interaction H_{int}.

The second order shifts that we require are obtained from (3.31) where the denominator does not contribute. In section 3 we examined the way that perturbation theory leads to energy shifts and obtained an understanding of which graphs contribute to the energy shift. With this understanding we may simplify the procedure and use instead an operator, matrix elements of which are the perturbative energy shifts we require.

If we include $\hat{H}_{int}(0)$ in the time evolution operator we get an operator expression

$$\lim_{\varepsilon \to 0^+} (-i) \int_{-\infty}^{0} dy^0 \, e^{-\varepsilon |y^0|} \, T\left[\hat{H}_{int}(0) \, \hat{H}_{int}(y^0) \right]. \qquad (5.1)$$

The only portion of $\hat{H}_{int}$ that will connect to our asymtotic states in this order is

$$\hat{H}_{int}(x^0) = -g \int d^3x \, \hat{\bar{\psi}}(x) \gamma_\mu \frac{\lambda^a}{2} \hat{\psi}(x) \hat{A}^\mu_a(x). \qquad (5.2)$$

inserting (5.2) in (5.1) we get

$$V = (-i)(-g)^2 (\gamma_\mu)_{\alpha'\alpha} (\gamma_\nu)_{\beta'\beta} (\lambda^a/2)_{c'c} (\lambda^b/2)_{d'd}$$
$$\int_{-\infty}^{0} dy^0 e^{-\varepsilon|y^0|} \int d^3x\, d^3y \, \langle 0|T[\hat{A}^\mu_a(x), \hat{A}^\nu_b(y)]|0\rangle$$
$$: \hat{\bar{\psi}}_{c'f'\alpha'}(x) \hat{\psi}_{cf\alpha}(x) \hat{\bar{\psi}}_{d'g'\beta'}(y) \hat{\psi}_{dg\beta}(y) : \quad . \qquad (5.3)$$

Here we have selected out a particular term from the Wick decomposition of (5.1) because only this term connects to external qq or $\bar{q}\bar{q}$ states in the way described by Fig 5.1 (a). If this is not obvious, a full evaluation of (3.31) can be used to give the same result.

Now we substitute in the cavity mode expansion (4.38) for the quark field operators, and the gluon propagator (4.46). There will be a number of terms with time dependence, but a simple rule exists for calculating the energy denominator. We have a state with unperturbed energy E_0, which may mix with an intermediate state with energy E_i. Including the -i from the expansion (3.10) for U we get the energy denominator

$$\frac{-1}{E_i - E_0} = (-i) \int_{-\infty}^{0} dt\, e^{-\varepsilon|t|} e^{i(E_i - E_0)t} \qquad (5.4)$$

We also change the ordering of the operators inside the normal ordering (an even number of swops). The resulting order will make the direct term positive, and the exchange term negative,

$$V = g^2 (\lambda^a/2)_{c'c} (\lambda^b/2)_{d'd} \delta_{f'f} \delta_{g'g}$$
$$(-\delta_{ab}) \, g^{\Sigma\Sigma}/2\Omega^\Sigma_m \, {}^{-1}/(\Omega^\Sigma_m + \varepsilon_{p'} - \varepsilon_p)$$
$$\int d^3x\, \bar{u}_{n'}(\underset{\sim}{x}) \gamma_\mu u_n(\underset{\sim}{x}) a^{\mu\Sigma}_m(\underset{\sim}{x})$$
$$\int d^3y\, \bar{u}_{p'}(\underset{\sim}{y}) \gamma_\nu u_p(\underset{\sim}{y}) a^{\nu\Sigma}_m(\underset{\sim}{y})$$
$$: a^\dagger_{c'n'} a^\dagger_{d'p'} a_{dp} a_{cn} : \qquad (5.5)$$

Now we insert for the vertex integrals Q^{Σ}_{nnm}/i as defined in Appendix A, and simultaneously absorb the $-\delta_{ab}$ from the gluon propagator to get

$$V = g^2 (\lambda^a/2)_{c'c} (\lambda^a/2)_{d'd} \delta_{f'f} \delta_{g'g} g^{\Sigma\Sigma}/2 \Omega^{\Sigma}_m {}^{-1}/(\Omega^{\Sigma}_m + \varepsilon_{n'} - \varepsilon_n)$$
$$Q^{\Sigma}_{n'nm} \tilde{Q}^{\Sigma}_{p'pm} a^{\dagger}_{c'n'} a^{\dagger}_{d'p'} a_{dp} a_{cn} . \qquad (5.6)$$

This expression may easily be understood by its correspondence with Fig 5.2.

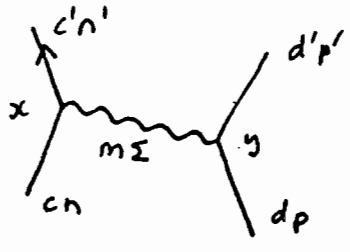

Fig 5.2 : Graphical representation of Eqn (5.6)

The calculation may easily be repeated for states consisting of qq. There are two ways of selecting a b as shown in Fig 5.3.

Fig 5.3 : One gluon exchange for $q\bar{q}$ systems

Relabelling makes the two diagrams of Fig 5.3 identical except for the energy denominators. In contrast to (5.6) we will now have $-\lambda^T/2$, after reordering the b $b^{\dagger}$ to make it the same as $a^{\dagger}$ a . The vertex integral of the antiquark will change in the signs of the quark cavity modes, and the quark labels will be transposed. Thus we get

$$V = g^2 \left(\lambda^a/2\right)_{c'c} \left(-\lambda^a/2\right)_{dd'} \delta_{f'f}\, \delta_{g'g}$$
$$g^{\Sigma\Sigma}/2\,\Omega^{\Sigma}_{m} \left[{}^{-1}/(\Omega^{\Sigma}_{m} + \varepsilon_{n'} - \varepsilon_{n}) + {}^{-1}/(\Omega^{\Sigma}_{m} + \varepsilon_{p'} - \varepsilon_{p}) \right]$$
$$Q^{\Sigma}_{n'nm}\ \tilde{Q}^{\Sigma}_{-p-p'm}\ a^{+}_{c'n'}\ b^{+}_{d'p'}\ b_{dp}\ a_{cn} \qquad (5.7)$$

The usual procedure is now to diagonalize the matrix of V in each degenerate subspace, in order to generate hyperfine splittings. In degenerate subspaces V is Hermitian, and thus the eigenvalues are real.

The remaining active ingredients of V are

$$g^{\Sigma\Sigma}/2\,\Omega^{\Sigma}_{m}\ Q^{\Sigma}_{n'nm}\ \tilde{Q}^{\Sigma}_{p'pm}$$
$$= \eta_{\Sigma}\ g^{\Sigma\Sigma}/2\,\Omega^{\Sigma}_{m}\ (-)^{M}\ Q^{\Sigma}_{n'nm}\ Q^{\Sigma}_{p'pm^*} \qquad (5.8)$$

The vertex integral can be split up into radial and angular integrals, as shown in Appendix A. If we absorb the parity selection rule into the radial integral we may define

$$S^{\Sigma}_{n'nm} = R^{\Sigma}_{n'nm}\ 1/2 \left(1 - g^{\Sigma\Sigma}\,\eta_{\Sigma}\,(-)^{\ell'+J+\ell}\right) \qquad (5.9)$$

The remaining portion of the angular integral gives

$$1/\hat{J}\ \ (4\pi)^{-1/2}\ (\hat{J}\ F_{JM}(n',n)) \qquad (5.10)$$

where

$$\hat{J} = \sqrt{2J+1}$$
$$F_{JM}(n'n) = (-)^{\mu'+1/2}\ \hat{j}'\,\hat{J}\,\hat{j} \begin{pmatrix} j' & J & j \\ 1/2 & 0 & -1/2 \end{pmatrix} \begin{pmatrix} j' & J & j \\ -\mu' & M & \mu \end{pmatrix} \qquad (5.11)$$

In summary

$$Q^{\Sigma}_{n'nm} = 1/\sqrt{4\pi}\ \ 1/\hat{J}\ S^{\Sigma}_{n'nm} \left(\hat{J}\, F_{JM}(n'n)\right) \qquad (5.12)$$

We finally see that

$$V = \alpha/R \; (\vec{\lambda}/2)_{c'c} \cdot (\vec{\lambda}/2)_{d'd} \sum_J V(J) \mu(J; n'np'p$$

$$a^+_{c'n'} \, a^+_{d'p'} \, a_{dp} \, a_{cn} \qquad (5.13)$$

where

$$V(J) = \sum_M (2J+1)(-)^M F_{JM}(n'n) \, F_{J-M}(p'p) \qquad (5.14)$$

$$\mu(J) = \sum_{N\Sigma} \eta_\Sigma \, g^{\Sigma\Sigma} \left(2\Omega^\Sigma_m (2J+1)\right)^{-1} S^\Sigma_{n'nm} \, S^\Sigma_{p'pm}$$

$$-1/(\Omega^\Sigma_m + \varepsilon_{n'} - \varepsilon_n) \qquad (5.15)$$

It can be shown that V(1) reduces to $\sigma_1 \cdot \sigma_2$ when acting on j=1/2 quarks. We now have a two body operator for the energy shift that is of the form

$$V = \sum_{ijkl} V_{ijkl} \; a^+_i a^+_j a_e a_k \qquad (5.16)$$

The label i is short for $c_i n_i$. V acts on basis vectors of the form

$$|i\rangle = a^+_3 a^+_4 |0\rangle$$

$$|f\rangle = a^+_1 a^+_2 |0\rangle \qquad (5.17)$$

The matrix element for the direct part will be

$$2V_{1234} \qquad (5.18)$$

and for the exchange part

$$-2V_{1243} \qquad (5.19)$$

The wavefunctions, that we will choose to operate on, are linear sums of antisymmetrized particle wavefunctions that are pure direct products of the various label spaces. The colour, flavour and (sometimes) angular momentum labels and operators may then be treated seperately.

If the angular momenta of the two particles making up a two particle state are the same then this space may be treated separately. The remaining orbital labels will either be symmetric, antisymmetric or identical. The term with orbital labels exchanged will then be added, subtracted or ignored respectively. If the angular momenta differ the fully antisymmetric wave function cannot be written as a single direct product in orbital and angular momentum space. The exchange must be added or subtracted based on the symmetry of the two spaces combined.

Later on we will need the second order perturbative shifts so we include the explicit numerical values for qq or $q\bar{q}$ in the lowest cavity modes

$$V = \alpha/R \; \vec{\lambda}_{1/2} \cdot \vec{\lambda}_{1/2} \left(\mu(0) + \underset{\sim}{\sigma}_1 \cdot \underset{\sim}{\sigma}_2 \mu(1) \right)$$

$$\mu(0) = 0.0098$$

$$\mu(1) = -0.1770 \qquad (5.20)$$

The one gluon annihilation process represented by Fig 5.1 (c) only affects $q\bar{q}$ states coupled to a colour octet with T=0 and J=1. It contributes an amount

$$V_A = \alpha/R \; (0.2813) \qquad (5.21)$$

5.2 4th Order Diagrams

We firstly construct all 4th order graphs connecting to asymptotic (anti)quark states. Firstly we observe that we get a class of diagrams simply by replacing the gluon lines in Fig 5.1 by the graphs shown in Fig 5.4.

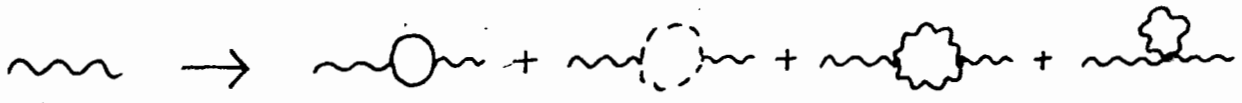

Fig 5.4 : Gluon self energy inserts

These graphs all diverge. In a plane wave basis, after renormalization, this results in the running coupling constant, which varies as a function of momentum. Such a renormalization program, although in principle possible, has not been carried out in the cavity. In our unrenormalized theory we simply treat the coupling constant as a constant.

In 4th order we will get several new self energy diagrams shown in Fig 5.5.

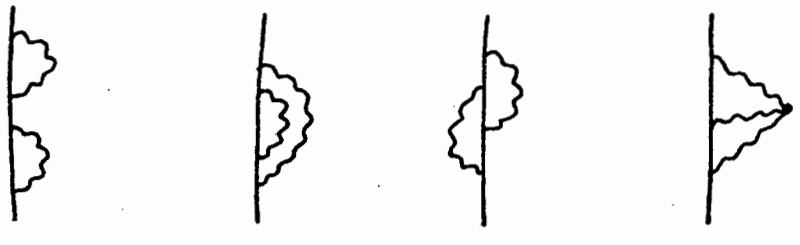

Fig 5.5 : Additional 4th order self energy diagrams

These diagrams will have the same effect as the diagram 5.1 (c). There will also be diagrams of the form shown in Fig 5.6, which we do not compute.

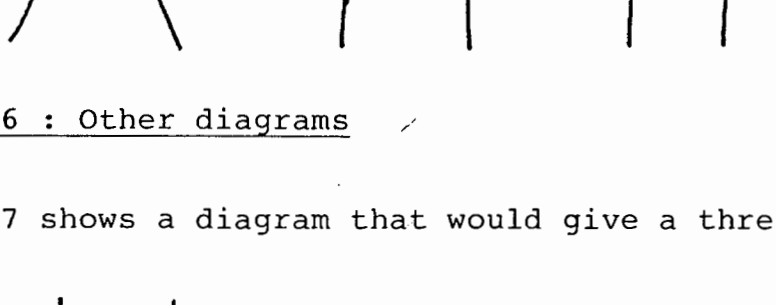

Fig 5.6 : Other diagrams

Fig 5.7 shows a diagram that would give a three body force.

Fig 5.7 : Three body force

Fig 5.8 shows the configuration mixing diagrams, we shall calculate the two body diagram.

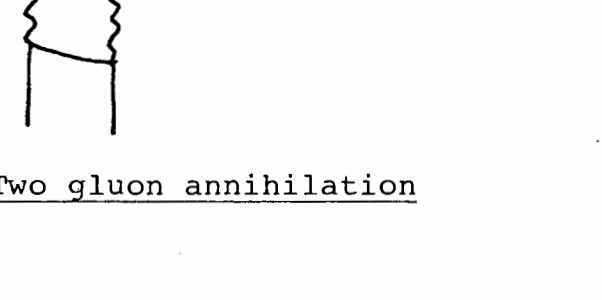

Fig 5.8 : Two and three body configuration mixing diagrams

Also of considerable interest is the two gluon annihilation shown in Fig 5.9 which is thought to be responsible for the splitting of the pseudoscalar mesons.

Fig 5.9 : Two gluon annihilation

5.3 Configuration Mixing Diagrams

The 4th order energy shift (g) is given by

$$\Delta E_k = (-i)^3/3! \int_{-\infty}^{0} dt_1 .. dt_3 \; e^{-\varepsilon(|t_1| + |t_2| + |t_3|)}$$

$$\langle \phi_k | T [\hat{H}_{int}(0) \hat{H}_{int}(t_1) .. \hat{H}_{int}(t_3)] | \phi_k \rangle_{ext\text{-}H \; conn} \qquad (5.22)$$

We include only that part of $\hat{H}_{int}$ given by (5.2), as we have already decided what graphs we wish to evaluate, namely those given by Fig 5.8.

In the above we have omitted the denominator of (3.31). The full expression is a power series in λ and is of the form

$$\Delta E = \frac{A\lambda^2 + B\lambda^4 + \ldots}{1 + C\lambda^2 + \ldots} \qquad (5.23)$$

where the coefficients A, B and C are given by

$$A = \langle \phi | \lambda \, H_{int} \, U^{(1)} | \phi \rangle_{ext\text{-}H \; conn}$$

$$B = \langle \phi | \lambda \, H_{int} \, U^{(3)} | \phi \rangle_{ext\text{-}H \; conn}$$

$$C = \langle \phi | U^2 | \phi \rangle_{ext \; conn} \qquad (5.24)$$

The superscript of U denotes the order of λ intended. Correct to order λ^5 we obtain

$$\Delta E = A\lambda^2 + (B - AC)\lambda^4 + \Theta(\lambda^5) \qquad (5.25)$$

We shall not show the term AC explicitly, but we simply note that it diverges in such a way as to cancel a divergence in B. The origin of the divergence becomes obvious when one looks at the explicit expansion. It is informative to compare this with the contents of section 3.3.

We start from the time ordered operator in (5.22), which is analogous to the operator in (5.1). Plugging in H and ignoring for the moment some factors we get

$$\int d\underset{\sim}{x}_1 \ldots d\underset{\sim}{x}_4 \int_{\infty}^{0} dx_2^0 \ldots dx_4^0$$

$$T\left[\bar{\psi}(x_1)\psi(x_1)\bar{\psi}(x_2)\psi(x_2)\bar{\psi}(x_3)\psi(x_3)\bar{\psi}(x_4)\psi(x_4)\right]$$

$$T\left[A(x_1)A(x_2)A(x_3)A(x_4)\right] \qquad (5.26)$$

We indicate one of the three possible ways of contracting the gluons among themselves. All are equivalent due to the symmetric appearance of x_2, x_3, x_4. We include a factor 3 and consider only the gluon contractions indicated.

The next step is to perform a Wick decomposition on the quark fields. We retain only those terms with a normal ordered product of four quark fields. These correspond to Fig 5.8 (a) and will be exact in a two quark system. In a three quark system we should also retain terms with six quark fields, corresponding to Fig 5.8 (b). We have not tackled these graphs.

We also ignore contractions that lead to self energy loops. For the time being we specialize to asymptotic states containing no antiquarks. Since $x_1^0 = 0$ is pinned down at a later time than all other times we know that we must have $\underset{\sim}{\psi}(x_1)$ but $\underset{\sim}{\bar{\psi}}(x_1)$ is not allowed.

The remaining possible contractions correspond to the labellings shown in Fig 5.10.

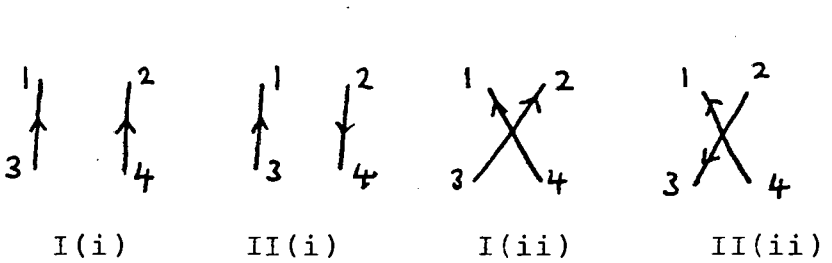

Fig 5.10 : The different contractions of (5.26)

We can immediately see that, provided that there is not simultaneous two gluon propagation, the sum of diagrams I(i) and I(ii) must antisymmetrize the intermediate two quark state. We may relabel I(ii) and II(ii) to make them identical to I(i) amd II(i) respectively, and thereby pick up a factor 2. After relabelling the diagrams appear as shown in Fig 5.11.

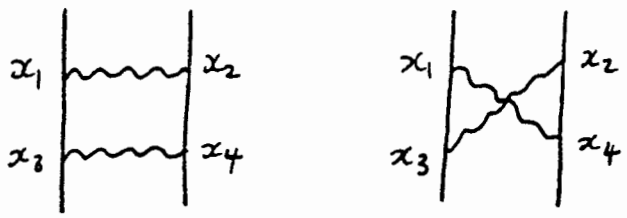

Fig 5.11 : Two types of configuration mixing diagrams

We now proceed to calculate I, in analogy to the second order case. The calculation will not be performed explicitly, but its correctness may be seen in correspondence with Fig 5.12. We also approximate here, by including only forward going n_5 and n_6 in (5.27). These should dominate, as other graphs are suppressed by their energy denominators.

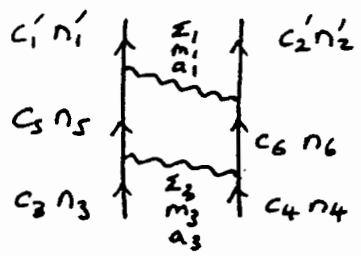

Fig 5.12 : Diagram corresponding to (5.27)

The 4th order energy shift operator W is given by

$$
\begin{aligned}
W_I \;=\; & 3\times 2\times \tfrac{1}{3!}\,(-g)^4 \\
& (\vec{\lambda}/2)_{c_1 c_5'}\cdot(\vec{\lambda}/2)_{c_2' c_6}\; g^{\Sigma_1\Sigma_1}/2\Omega_1\; Q^{\Sigma_1}_{n_1' n_5 m_1}\,\tilde{Q}^{\Sigma_1}_{n_2' n_6 m_1} \\
& (\vec{\lambda}/2)_{c_5 c_3}\cdot(\vec{\lambda}/2)_{c_6 c_4}\; g^{\Sigma_3\Sigma_3}/2\Omega_3\; Q^{\Sigma_3}_{n_5 n_3 m_3}\,\tilde{Q}^{\Sigma_3}_{n_6 n_4 m_3} \\
\Big[\; & (-)(\Omega_3+\varepsilon_6-\varepsilon_4)^{-1}\,(-)(\varepsilon_5+\varepsilon_6-\varepsilon_3-\varepsilon_4)^{-1}(-)(\Omega_1+\varepsilon_5-\varepsilon_{1'})^{-1}+ \quad \leftarrow \text{Ia} \\
& (-)(\Omega_3+\varepsilon_5-\varepsilon_3)^{-1}\,(-)(\varepsilon_5+\varepsilon_6-\varepsilon_3-\varepsilon_4)^{-1}(-)(\Omega_1+\varepsilon_5-\varepsilon_{1'})^{-1}+ \quad \leftarrow \text{Ib} \\
& (-)(\Omega_3+\varepsilon_6-\varepsilon_4)^{-1}(-)\,(\varepsilon_{2'}-\varepsilon_4+\Omega_1+\Omega_3)^{-1}(-)(\Omega_1+\varepsilon_5-\varepsilon_1)^{-1}\Big] \quad \leftarrow \text{Ic} \\
& a_{1'}^{+}\, a_{2'}^{+}\, a_4\, a_3 \,. \qquad (5.27)
\end{aligned}
$$

We have condensed slightly the notation used in 2nd order in an obvious way (cf (5.6)). For example ε_1 and Ω_1 are short for ε_{n_1} and $\Omega^{\Sigma_1}_{m_1}$. The energy denominator may be read off from Fig 5.13. where we have used that

$$\varepsilon_1+\varepsilon_2 = \varepsilon_3+\varepsilon_4 \,. \qquad (5.28)$$

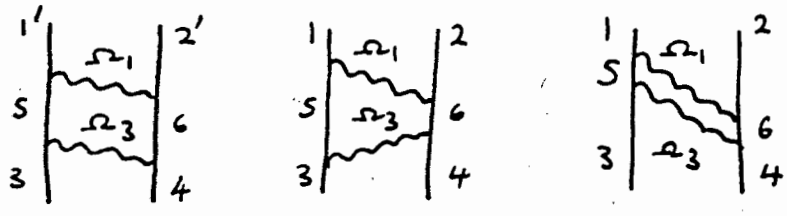

Ia Ib Ic

Fig 5.13 : Time ordered diagrams for energy denominators

The sum over the quark labels 5 and 6 may be replaced

$$\sum_{56} f(5,6)\,g(5,6) = \sum_{56\,5'6'} f(5,6)\,g(5',6')\,\delta_{55'}\,\delta_{66'} \,. \qquad (5.29)$$

f and g represent different parts of W. We perform this insertion and associate the primed labels with the Ω_3 gluon. For the time being we ignore the Ic denominator.

$$W_{Ia,Ib} = g^4 \; {}^{-1}\!/(\varepsilon_5+\varepsilon_6-\varepsilon_3-\varepsilon_4)$$
$$(\lambda^{a_1}/2)_{c_1'c_5} (\lambda^{a_1}/2)_{c_2'c_6} \; Q^{\Sigma_1}_{n_1'n_5 m_1} \widetilde{Q}^{\Sigma_1}_{n_2'n_6 m_1} \; {}^{-1}\!/(\Omega_1+\varepsilon_5-\varepsilon_1')$$
$$(\lambda^{a_3}/2)_{c_5'c_3} (\lambda^{a_3}/2)_{c_6'c_4} \; Q^{\Sigma_3}_{n_5'n_3 m_3} \widetilde{Q}^{\Sigma_3}_{n_6'n_4 m_3}$$
$$\left({}^{-1}\!/(\Omega_3+\varepsilon_6'-\varepsilon_4) + {}^{-1}\!/(\Omega_3+\varepsilon_5'-\varepsilon_3)\right) \delta_{5'5}\,\delta_{6'6}\, a_1^\dagger a_2^\dagger a_4 a_3 \qquad (5.30)$$

We observe that

$$\sum_M Q^{\Sigma}_{n'nm} \widetilde{Q}^{\Sigma}_{p'pm} = \sum_M \widetilde{Q}^{\Sigma}_{n'nm} Q^{\Sigma}_{p'pm} \qquad (5.31)$$

Using the above, and swopping labels 3 with 4, and 5 with 6, we may replace

$$\delta_{5'5}\,\delta_{6'6} \rightarrow \tfrac{1}{2}\left(\delta_{55'}\delta_{66'} - \delta_{56'}\delta_{65'}\right) \qquad (5.32)$$

We note that

$$\delta_{55'}\delta_{66'} - \delta_{56'}\delta_{65'} = \tfrac{1}{2}\sum_{11,12}\left(\delta_{5\,11}\delta_{6\,12} - \delta_{5\,12}\delta_{6\,11}\right)\left(\delta_{11\,5'}\delta_{12\,6'} - \delta_{11\,6'}\delta_{12\,5'}\right) \qquad (5.33)$$

This resembles

$$a_4 a_3 a_1^\dagger a_2^\dagger |0\rangle = \left(\delta_{13}\delta_{24} - \delta_{14}\delta_{23}\right) \qquad (5.34)$$

So that we may think of 11, 12 as being a complete set of intermediate qq states that we sum over. What we now get for the matrix elements of W is

$$\langle 12 | W_{Iab} | 12\rangle = \sum_{11,12} \tfrac{1}{2} \; {}^{-1}\!/(\varepsilon_{11}+\varepsilon_{12}-\varepsilon_1-\varepsilon_2)$$
$$\langle 11\;12|V|12\rangle\langle 11\;12|V|1\;2\rangle \qquad (5.35)$$

Now we can see that this term contains a divergence in the case that $\varepsilon_5+\varepsilon_6 = \varepsilon_1+\varepsilon_2$. There could be a variety of such degenerate states. If we have diagonalized V in the degenerate subspace there will be only one state that will be connected by V . (If the degeneracy is not lifted in this order the diagonalization is trivial.) It is precisely this divergence that is cancelled by the term AC in (5.25).

The first term is in pleasing correspondence with the 2nd order perturbation expression in elementary quantum physics, i.e.

$$\Delta E^{(2)} = - \sum_{n \neq i} \frac{V_{in}^{*} V_{ni}}{E_n - E_i} \qquad (5.36)$$

This acts as a check of overall sign.

With the aid of Fig 5.14 we may write down II,

$$W_{II} = g^4$$
$$(\lambda^{a_1}/2)_{c_1' c_5} (\lambda^{a_3}/2)_{c_5 c_3} (\lambda^{a_3}/2)_{c_5 c_3} (\lambda^{a_1}/2)_{c_6 c_4}$$
$$g^{\Sigma_1 \Sigma_1'/2\Omega_1} g^{\Sigma_3 \Sigma_3'/2\Omega_3} Q^{\Sigma_1}_{n_1' n_5 m_1} \tilde{Q}^{\Sigma_3}_{n_2' n_6 m_3} Q^{\Sigma_3}_{n_5 n_3 m_3} \tilde{Q}^{\Sigma_1}_{n_6 n_4 m_1}$$
$$\Big[(-)(\Omega_1+\varepsilon_6-\varepsilon_4)^{-1} (-)(\Omega_1+\Omega_3+\varepsilon_5+\varepsilon_6-\varepsilon_3-\varepsilon_4)^{-1} (-)(\Omega_1+\varepsilon_5-\varepsilon_1')^{-1} \quad \leftarrow \text{II a}$$
$$+ \; (-)(\Omega_1+\varepsilon_5-\varepsilon_3)^{-1} (-)(\Omega_1+\Omega_3+\varepsilon_5+\varepsilon_6-\varepsilon_3-\varepsilon_4)^{-1} (-)(\Omega_3+\varepsilon_5-\varepsilon_1')^{-1} \quad \leftarrow \text{II b}$$
$$+ \; (-)(\Omega_1+\varepsilon_6-\varepsilon_4)^{-1} (-)(\Omega_1+\Omega_3+\varepsilon_2'-\varepsilon_4)^{-1} (-)(\Omega_1+\varepsilon_5-\varepsilon_1')^{-1} \Big] \quad \leftarrow \text{II c}$$
$$a_1^{+}, a_2^{+}, a_4 a_3 \qquad (5.37)$$

Fig 5.14 : Diagram corresponding to (5.36)

We may conveniently group together Ic and IIc,

$$
\begin{aligned}
W_{Ic+IIc} \;=\; & g^4\, g^{\Sigma_1\Sigma_1'}/2\Omega_1\; g^{\Sigma_2\Sigma_2'}/2\Omega_2 \\
& (\lambda^{a_1}/2)_{c_1'c_5}\,(\lambda^{a_2}/2)_{c_2'c_6}\; Q^{\Sigma_1}_{n_1'n_5 m_1}\; \tilde{Q}^{\Sigma_2}_{n_2'n_6 m_2} \\
& (\lambda^{a_3}/2)_{c_5c_3}\,(\lambda^{a_4}/2)_{c_6c_4}\; Q^{\Sigma_3}_{n_5n_3m_3}\; \tilde{Q}^{\Sigma_4}_{n_6n_4m_4} \\
& \left[\, {}^{-1}/(\varepsilon_6+\Omega_4-\varepsilon_4)\;{}^{-1}/(\Omega_1+\Omega_4+\varepsilon_2'-\varepsilon_4)\;{}^{-1}/(\Omega_1+\varepsilon_5-\varepsilon_1')\,\right] \\
& \left[\delta_{12}\delta_{34}+\delta_{14}\delta_{23}\right]^{a\,m\,\Sigma} \\
& a_1^\dagger\, a_2^\dagger\, a_4\, a_3
\end{aligned}
\qquad (5.38)
$$

In this form the bosonic symmetry of the intermediate two gluon state is apparent. The quarks do not need to be antisymmetrized, as they do not propagate simultaneously.

5.4 Two Gluon Annihilation

So far, we have restricted ourselves to qq or $q\bar{q}$ asymptotic states. $q\bar{q}$ states, in addition to all the processes described above, may annihilate into two gluons is they are in a colour singlet. Calculation of this process proceeds along similar lines to two gluon exchange.

Ignoring self energies, and restricting ourselves to $q\bar{q}g$ and gg intermediate states we obtain

$$
\begin{aligned}
V = {} & g^4 \left(\lambda^{a_1}/2\right)_{c_1 c_5} \left(\lambda^{a_2}/c_5 c_2\right) \\
& \left[g^{\Sigma_1 \Sigma_1}/2\Omega_1 \; g^{\Sigma_2 \Sigma_2}/2\Omega_2 \left(-1/(\Omega_1 + \Omega_2 - \varepsilon_3 - \varepsilon_4) \right) \right] \\
& \left[Q^{\Sigma_1}_{n_1 n_5 m_1} Q^{\Sigma_2}_{n_5 n_2 m_2} \frac{-1}{\Omega_1 + \varepsilon_5 - \varepsilon_1} - Q^{\Sigma_1}_{n_1 - n_5 m_1} Q^{\Sigma_2}_{-n_5 - n_2 m_2} \frac{-1}{\Omega_2 + \varepsilon_5 - \varepsilon_2} \right] \\
& \left[\delta_{13}\delta_{24} + \delta_{14}\delta_{23} \right]^{a m \Sigma} \\
& \left[\tilde{Q}^{\Sigma_4}_{-n_4 n_6 m_4} \tilde{Q}^{\Sigma_3}_{n_6 n_3 m_3} \frac{-1}{\Omega_3 + \varepsilon_6 - \varepsilon_3} - \tilde{Q}^{\Sigma_4}_{-n_4 - n_6 m_4} \tilde{Q}^{\Sigma_3}_{-n_6 n_3 m_3} \frac{-1}{\Omega_4 + \varepsilon_6 - \varepsilon_4} \right] \\
& \left(\lambda^{a_4}/2\right)_{c_4 c_6} \left(\lambda^{a_3}/2\right)_{c_6 c_3} \\
& a_1^{+} \, b_2^{+} \, b_4 \, a_3
\end{aligned}
\tag{5.39}
$$

This expression may be seen to be in correspondence to Fig 5.15.

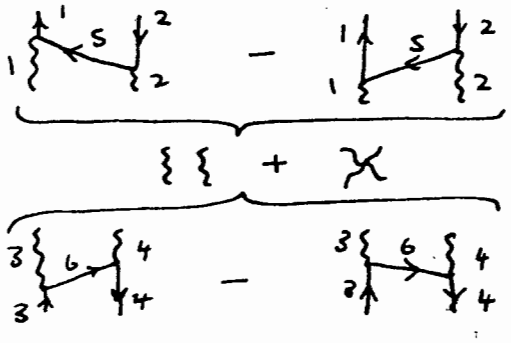

Fig 5.15 : Two gluon annihilation

We now introduce

$$|i\rangle = a^{\dagger}_{c_1 n_1}\, b^{\dagger}_{c_2 n_2}\, |0\rangle \tag{5.40}$$

$$|j\rangle = c^{\Sigma_7 \dagger}_{a_7 m_7}\, c^{\Sigma_8 \dagger}_{a_8 m_8} \tag{5.41}$$

After some manipulation

$$\langle i|U|i\rangle = \sum_j \tfrac{1}{2} \left(-g^{\Sigma_7 \Sigma_7}\right)\left(-g^{\Sigma_8 \Sigma_8}\right) B_{ij}^2 \; {}^{-1}\!/_{(\Omega_7+\Omega_8-\varepsilon_1-\varepsilon_2)} \tag{5.42}$$

where Bij, a real number, is

$$B_{ij} = \sum_{c_5 n_5} \sum_{\substack{a_1 m_1 \\ a_2 m_2}} g^2 \left(\lambda^{a_1}/2\right)_{c_1 c_5} \left(\lambda^{a_2}/2\right)_{c_5 c_2} \left[Q^{\Sigma_1}_{n_1 n_5 m_1} Q^{\Sigma_2}_{n_5 - n_2 m_2} \frac{-1}{\Omega_1 + \varepsilon_5 - \varepsilon_1} - Q^{\Sigma_1}_{n_1 - n_5 m_1} Q^{\Sigma_2}_{-n_5 - n_2 m_2} \frac{-1}{\Omega_2 + \varepsilon_5 - \varepsilon_2} \right] \sqrt{2\Omega_1 2\Omega_2} \left(\delta_{17}\delta_{28} + \delta_{18}\delta_{27}\right) a m \Sigma \tag{5.43}$$

Thus, similar to (5.34) we have the 4th order contribution. The g.. is a new, but not unexpected contribution. It means that despite the fact that i is lower in energy than j, if j contains one scalar gluon it will <u>raise</u> the energy of i as the interaction is turned on. This surprising phenomenon is due to the fact that our Hilbert space has an indefinite metric.

6 RESULTS

6.1 Configuration Mixing

In order to understand the configuration mixing results, one should firstly look at the quark and gluon energy level spectra in a spherical cavity, as shown in Table 6.1. The closest energy levels to 1s1/2 are 1p3/2 and 1p1/2, and on this basis we might expect that they might play the dominant role in configuration mixing.

We also introduce some terminology; the I and II portions of the W operator of the previous chapter we refer to as 'straight' and 'crossed' respectively. This is simply a convenient distinction based on the appearance of Fig 5.11.

At this point we should also stress that our interactions are dynamic. In a (non-relativistic) theory of instantaneous interactions the graphs Ic, IIabc would not be present.

The mathematical structure of straight and crossed graphs is quite distinct. The straight graphs Iab can always be broken up into the product of two single gluon exchanges, and an additional energy denominator for the intermediate two quark state.

As an aid to interpreting our results we introduce some basic perturbation theory. Consider the Hamiltonian

$$H = H_0 + \lambda V \tag{6.1}$$

H_0 has eigenstates ϕ_0, ϕ_1 with energies W_0 and W_1. The perturbed wave function (Sc 68) is

$$\begin{aligned} \psi &= \phi_0 + \beta \phi_1 \\ &= \phi_0 - \lambda \frac{\langle \phi_1 | V | \phi_0 \rangle}{W_1 - W_0} \phi_1 \end{aligned} \tag{6.2}$$

Table 6.1 : Quark and gluon eigenenergies

Massless quarks

KAPPA

N	-5	-4	-3	-2	-1	1	2	3
1	6.518	5.430	4.327	3.204	2.043	3.812	5.123	6.371
2	10.556	9.322	8.060	6.758	5.396	7.002	8.408	9.754
3	14.012	12.710	11.377	10.004	8.578	10.163	11.612	13.009

Gluons

Magnetic
Electric
Longitudinal/Scalar

	J=0	J=1	J=2	J=3	J=4	J=5
N=1		2.744	3.870	4.973	6.062	7.140
		4.493	5.763	6.988	8.183	9.356
	4.493	2.082	3.342	4.514	5.647	6.756
N=2		6.117	7.443	8.722	9.968	11.189
		7.726	9.095	10.417	11.705	12.967
	7.725	5.940	7.290	8.584	9.840	11.070
N=3		9.317	10.713	12.064	13.380	14.670
		10.904	12.323	13.698	15.040	16.355
	10.904	9.206	10.614	11.973	13.296	14.591

where β is the probability amplitude of ϕ_1 in Ψ. Ψ is not normalized.

The perturbed energy is

$$E = W_0 + \Delta E^{(1)} + \Delta E^{(2)}$$

$$= W_0 + \lambda \langle \phi_0 | V | \phi_0 \rangle - \lambda^2 \frac{\langle \phi_0 | V | \phi_1 \rangle \langle \phi_1 | V | \phi_0 \rangle^*}{W_1 - W_0} \qquad (6.3)$$

One of the necessary conditions for perturbation theory to be valid is that

$$|\beta|^2 \ll 1 \qquad (6.4)$$

In other words the character of the initial state is not appreciably changed by the perturbation. Another expression for $|\beta|^2$ is

$$|\beta|^2 = \left| \Delta E^{(2)} / W_1 - W_0 \right| \qquad (6.5)$$

As an example we let V correspond to H_{int}, and consider one gluon exchange. As previously calculated

$$\Delta E^{(2)} = \alpha/R \ \vec{F}_1 \cdot \vec{F}_2 \ \sum_J \mu(J) V(J) \qquad (6.6)$$

For two 1s1/2 quarks coupled to 0^+ in a colour anti-triplet the energy shift from the 1M1 gluon (2.74) is

$$\Delta E^{(2)} \doteq \alpha/R \ (-2/3)(-.1770)(-3)$$

$$\doteq \alpha/R \ -0.35 \qquad (6.7)$$

Therefore

$$|\beta|^2 \doteq \alpha \ 0.13 \qquad (6.8)$$

The pion will have qq in a colour singlet, so

$$|\beta|^2 = \alpha \quad 0.26 \tag{6.9}$$

In this regime of $|\beta|^2$ we cannot expect accurate results, but hopefully the general trends will be reliable. If there is a near degeneracy of W_o and W_1, a far more accurate result will be obtained by the use of degenerate perturbation theory, i.e. by diagonalizing H in the subspace of ϕ_o and ϕ_1. The accuracy of this result will be determined by how well the system can be described in the truncated Hilbert space.

We firstly present some results for the straight portions Iab. In equation (5.34) it was shown that

$$\Delta E_{Iab}(i) = \langle i | W_{Iab} | i \rangle = -\sum_j \frac{\langle j|V|i\rangle\langle j|V|i\rangle}{E(j) - E(i)}$$

$$= W_{ii} = -\sum_j V_{ij}^2 / E(j) - E(i) \tag{6.10}$$

i is the initial state, and j an intermediate state. The intention is to calculate the energy shift of i due to each j. Table 6.2 shows an explicit calculation of this quantity where the state i is a two quark system coupled to J=0, parity +. In the first column the orbital quantum numbers of the intermediate two quark state j are shown. The second column shows the one gluon exchange matrix element Vij, excluding the $\alpha_s \vec{F}_1 . \vec{F}_2$ portion, and summed over all possible intermediate gluons. This number may be compared with Vii. By including the relevant colour factor (see Table 6.4), this table may be applied to all possible colour representations of qq or qq states. The third column shows the energy shift due to each intermediate two quark state, which must still be multiplied by $(\vec{F}_1 . \vec{F}_2)^2 \alpha^2 / R$. The final column, lacking the same factor, shows a quantity corresponding to $|\beta|^2$. The correspondence is obtained by considering V of (6.1) as a product of two H_{int} operators, i.e. one gluon exchange. One should of course recall that one (physical) gluon exchange is a dynamic process and that a portion of the wavefunction will now contain some qqg admixture corresponding to this process, in the case of physical gluons.

Table 6.2 : Detailed results of W Iab

State i : Two 1s1/2 quarks coupled to j=0, parity +.
State j : Intermediate state of two quarks with n, kappa as shown.

F=E(i) - E(j)

Vij = (j | $\Sigma\mu$(J) V(J) | i)

State j				Vij	$(Vij)^2 / F$	$(Vij/F)^2$
N1	K1	N2	K2			
1	-1	1	-1	0.540843		
1	-2	1	-2	-1.011124	-0.4402485	0.189577
1	-3	1	-3	0.507277	-0.0563205	0.012327
1	-4	1	-4	-0.326925	-0.0157792	0.002330
1	-5	1	-5	0.234934	-0.0061668	0.000689
1	-6	1	-6	-0.179889	-0.0029135	0.000262
1	-7	1	-7	0.143683	-0.0015582	0.000118
1	-8	1	-8	-0.118300	-0.0009100	0.000059
1	-9	1	-9	0.068194	-0.0002657	0.000015
2	-1	2	-1	0.186595	-0.0051916	0.000774
3	-1	3	-1	0.064585	-0.0003192	0.000024
4	-1	4	-1	0.017384	-0.0000156	0.000001
5	-1	5	-1	0.000078	0.0000000	0.000000
1	1	1	1	-0.357909	-0.0362117	0.010237
1	2	1	2	0.195312	-0.0061920	0.001005
2	1	2	1	-0.085939	-0.0007446	0.000075
1	-1	2	-1	0.085849	-0.0021979	0.000655

It can be seen that the radial excitations mix very weakly. This is is largely due to the rapid falling off of the radial integrals. The modes that mix most strongly are the maximally stretched modes, the lp3/2, ld5/2, ... In fact the matrix element for $(1s1/2)^2-(1p3/2)^2$ is nearly double that of the $(1s1/2)^2-(1s1/2)^2$ matrix element.

We note further that the $(1s1/2)^2-(1p3/2)^2$ transition proceeds via J=1 and J=2 gluons with negative parity . The largest part of this is due to 1S1 and 1L1 gluons. In other words the transition is due to the colour Coulomb interaction. We should add that after projection of our perturbed wave function onto the physical subspace there will be no contribution to physical wave function corresponding to the presence of unphysical gluons.

These results may also be contrasted with the original MIT results, where the Coulomb portion of the interaction was found to have an almost negligable effect, in comparison to the spin-spin splittings. The reason for this is not hard to find, (at least in the Feynman gauge formulation of the field theory with a subsidiary condition). The Jp=0+ 1S0 gluon radial distribution, which carries the Coulomb interaction in second order, has a zero, whereas the 1- 1S1 gluon has a radial distribution nicely shaped to cause strong radial matrix elements with the nu=1, kappa=-1, -2, ... quark states.

The results in the 1- case are similar, roughly in the ratio of 0-:1- is 1:2 to 1:3, as opposed to the previous 1:-3 of the hyperfine interaction.

One may ask what effect the admixture of these excited states may have on the consistency of the spherical bag assumption. Each individual quark exerts a non-spherical pressure on the bag. Parity and angular momentum considerations force the excited states always to have the identical orbital quantum numbers, when coupled to J=0. From the viewpoint of pressure the particles are

therefore indistinguishable. Any state with two such particles coupled to zero angular momentum will have net spherical pressure. Of course, provided that the admixture is small, we may tolerate states with non-spherical pressure (e.g. (1p3/2) coupled to 1+), without upsetting the consistency of the spherical bag picture too much.

The convergence is sufficiently fast that an accurate result could be obtained for the perturbation theory value of W Iab. The result would loose validity as $|\beta|^2$ became comparable to 1. For example the pion would have

$$|\beta|^2 \doteq \alpha \; 0.34 \tag{6.11}$$

for the intermediate (1p3/2) state.

Thus we see that for the pion the notion of our perturbation theory being valid is dubious for α of order 1. As the perturbation theory breaks down it will overestimate the strength of the energy shift due to the $(1p3/2)^2$ state. Other effects may also come into play. If the pion has a more collective nature, as suggested in (Ge 86), then the energy shift is likely to be strong.

All these states will have admixtures of (physical) qqg. Strictly (6.4) should be replaced by a condition

$$\sum_i |\beta_i|^2 << 1 \tag{6.12}$$

where the sum is over all possible intermediate states.

We point out that this admixture of qqg states is a troublesome complication to the problem. In an problem with (nearly) instantaneous interactions one might have followed a Tamm-Dancoff approach. Steps toward the generalization of this technique to problems with dynamic interactions have been made (Ge 86). A simple approach would consist of diagonalizing the Hamiltonian in

a truncated basis. This option is not legitimately available to us, without regularising the divergence of the self energy.

We now briefly consider the use of perturbation theory for excited states. The dynamic nature of the gluon is reflected in the non-hermiticity of matrix elements of V taken between left and right two quark states of different energy. This is because one gluon exchange is energy dependent, and the resulting energy denominator favours transitions downwards from higher levels because the intermediate gluon has to borrow less energy.

Table 6.3 shows perturbations on various initial states due to W Iab. We perturb the initial state in column one, via the intermediate state in column two. The conventions for $\mathcal{K}$ and $\vec{F}_1.\vec{E}_2$ apply as for Table 6.2. The 4th order perturbative energy shift is shown in the final column. (The states indicated x2 must be counted twice.) The results show that the excited states show a strong upward push from the lower states. The strength of the shifts suggests that perturbation theory breaks down at a far lower than for ground states.

We already know that the ground states have strong admixtures for α =1, this is even more significant for the excited states. At this stage, because of this behaviour we do not pursue this topic.

We now describe the calculation of the crossed graphs. The familiar $\vec{\lambda}_1.\vec{\lambda}_2$ or $\underset{\sim}{\sigma}_1.\underset{\sim}{\sigma}_2$ have now been replaced by mathematically distinct operators. In two body interactions we have already generalized $\underset{\sim}{\sigma}_1.\underset{\sim}{\sigma}_2$ to V(J), so that we can deal with cases other than spin 1/2 quarks, and spin 1 gluons. For convenience we split the expressions for W into their colour, angular momentum and radial parts. Each part is evaluated separately and the results combined in such a way as to respect the permutation symmetry.

The angular momentum part of the crossed graph is, for some specific internal quark and gluon angular momentum

Table 6.3 : W Iab for ground and excited states

All sums truncated at the 2% level.

Initial state J=0		2nd Order	Intermediate State		4th Order	
1s1/2	1s1/2	0.5408				
			1p3/2	1p3/2	-0.4402	
			1d5/2	1d5/2	-0.0563	
			1f7/2	1f7/2	-0.0158	
			1p1/2	1p1/2	-0.0362	
					-0.5484	
1p3/2	1p3/2	1.0073				
			1s1/2	1s1/S	3.1856	
			1d5/2	1d5/2	-0.8447	
			1f7/2	1f7/2	-0.1277	
					2.2132	
1p1/2	1p1/2	0.4841				
			1s1/2	1s1/2	1.9556	
			1p3/2	1p3/2	0.0751	
			1d3/2	1d3/2	-0.2718	
			2s1/2	2s1/2	-0.0494	
					1.7095	

Initial state J=1		2nd Order	Intermediate State		4th Order	
1s1/2	1s1/2	-0.1672				
			1p3/2	1p3/2	-0.0985	
			1d5/2	1d5/2	-0.0075	
			1f7/2	1f7/2	-0.0016	
			1p1/2	1p1/2	-0.0040	
			1p3/2	1p1/2	-0.0226	x 2
					-0.1568	
1p3/2	1p1/2	0.2020				
			1s1/2	1s1/2	3.0738	
1d5/2	1s1/2	0.2080				
			1p3/2	1p3/2	0.2976	
			1p3/2	1p1/2	0.7260	x 2
			1p1/2	1p1/2	-0.1249	
					1.6247	
1p3/2	1p3/2	0.2849				
			1s1/2	1s1/S	1.7698	
			1d5/2	1d5/2	-0.3171	
			1f7/2	1f7/2	-0.0312	
			1p3/2	1p1/2	-0.0139	x 2
					1.3937	
1p1/2	1p1/2	0.0148				
			1s1/2	1s1/2	0.2173	
			1p3/2	1p3/2	0.0096	
			1d3/2	1d3/2	-0.0026	
					0.2243	

$$\sum_{M_1 M_2} (2J_1+1)(2J_2+1)\,(-)^{M_1+M_2}$$

$$F_{J_1 M_1}(n_1 n_5)\; F_{J_2 -M_2}(n_2 n_6)$$

$$F_{J_2 M_2}(n_5 n_3)\; F_{J_1 M_1}(n_6 n_4)$$

$$a^{\dagger}_{n_1}\, a^{\dagger}_{n_2}\, a_{n_4}\, a_{n_3} \qquad (6.13)$$

We calculate matrix elements of this operator between states of good angular momentum by computer, but as a check we consider a special case. The straight graph, in the case of j=1/2 quarks, is simply

$$(\underset{\sim}{\sigma_1} \cdot \underset{\sim}{\sigma_2})^2 = 3 - 2\, \underset{\sim}{\sigma_1} \cdot \underset{\sim}{\sigma_2} \qquad (6.14)$$

It is not hard to show using the (anti) commutation relations for the σ's, that the crossed graph crossed graph expression reduces

$$\sigma_{1i}\, \sigma_{1j}\, \sigma_{2j}\, \sigma_{2i} = -(\underset{\sim}{\sigma_1} \cdot \underset{\sim}{\sigma_2})^2 + 6$$

$$= 3 + 2\, \underset{\sim}{\sigma_1} \cdot \underset{\sim}{\sigma_2} \qquad (6.15)$$

This gives a useful check on the computer code. As a further check we calculate the straight graph with the same code, and check it against $V(J)^2$.

The operator expression for the crossed graphs in colour space acting on a qq system is

$$(\lambda^{a_1}/2)_{c_1 c_5}\, (\lambda^{a_2}/2)_{c_2 c_6}\, (\lambda^{a_2}/2)_{c_5 c_3}\, (\lambda^{a_1}/2)_{c_6 c_4}\, a^{\dagger}_{c_1} a^{\dagger}_{c_2}\, a_{c_4} a_{c_3} \qquad (6.16)$$

The straight graph is

$$\left[(\lambda^{a_1}/2)_{c_1 c_3}\, (\lambda^{a_1}/2)_{c_2 c_4}\right]^2 a^{\dagger}_{c_1}\, a^{\dagger}_{c_2}\, a_{c_4}\, a_{c_3} \qquad (6.17)$$

In a condensed notation

$$\left(\vec{\lambda}_1/2 \cdot \vec{\lambda}_2/2\right)^2 \qquad (6.18)$$

In qq systems we would write

$$\left(\vec{\lambda}_1/2 \cdot -\vec{\lambda}_2^T/2\right)^2 \qquad (6.19)$$

Using the commutation relations of the colour generators and the fact that

$$\sum_{j,k=1}^{8} f_{ijk} f_{ijk} = 3 \qquad i = 1..8 \qquad (6.20)$$

where the f_{ijk} are the SU(3) structure constants, it can be shown that the crossed colour graph for qq is

$$\left(\vec{\lambda}_1/2 \cdot \vec{\lambda}_2/2\right)^2 + 3/2\left(\vec{\lambda}_1/2 \cdot \vec{\lambda}_2/2\right) \qquad (6.21)$$

For the case of qq we have similarly

$$\left(\vec{\lambda}_1/2 \cdot -\vec{\lambda}_2^T/2\right)^2 + 3/2\left(\vec{\lambda}_1/2 \cdot -\vec{\lambda}_2^T/2\right) \qquad (6.22)$$

These results were cross-checked by explicit computer calculation, and results are shown in Table 6.4 in column 3.

Having evaluated the colour and angular momentum factors we may proceed with the full evaluation of W Iabc and IIabc. Table 6.5 shows some sample results of such a calculation. We display results for only the ground state, i.e. two 1s1/2 states coupled to J=0 and J=1. Only contributions greater than 2% of the largest value are shown.

The values in the table must be multiplied by α^2/R, and by the appropriate colour factors in Table 6.4, for use in qq and $q\bar{q}$ systems. We note that the Iab portion dominates to a greater or lesser extent in both cases.

Table 6.4 : Colour and Angular momentum factors

Colour Representation	$F_1.F_2$	$(F_1.F_2)^2$	crossed graph	2 gluon straight	2 gluon crossed
Anti-triplet	-2/3	4/9	-5/9		
Sextet	1/3	1/9	11/18		
Singlet	-4/3	16/9	-2/9	2/3	2/3
Octet	1/6	1/36	5/18	21/36	-1/6
Spin Representation	$\sigma_1.\sigma_2$	$(\sigma_1.\sigma_2)^2$	crossed graph	2 gluon straight	2 gluon crossed
Singlet	-3	9	-3	6	6
Triplet	1	1	5	4	-4

Table 6.6 : Convergence of W Iab

Initial state : Two massless 1s1/2 states coupled to J=0
All sums are carried out over quark and gluon radial quantum numbers up to M.

kappa	M=1	M=2	M=3
4	-0.000616		
3	-0.001552	-0.000541	
2	-0.005337	-0.001268	-0.000160
1	-0.035935	-0.001167	-0.000126
-1	-0.000000	-0.009585	-0.000437
-2	-0.435765	-0.008385	-0.000521
-3	-0.055654	-0.002499	-0.000296
-4	-0.015591	-0.001181	
-5	-0.006096		
-6	-0.002881		
-7	-0.001542		

Initial state : Two mass=1.5 1s1/2 states coupled to J=0

kappa	M=1	M=2	M=3
4	-0.000801		
3	-0.002259	-0.001152	
2	-0.008885	-0.003059	-0.000419
1	-0.071503	-0.007418	-0.000416
-1	0.000000	-0.022085	-0.001028
-2	-0.339568	-0.031325	-0.001298
-3	-0.036628	-0.006129	-0.000661
-4	-0.009247	-0.002234	
-5	-0.003353		
-6	-0.001495		
-7	-0.000763		

We also note the appearance of (1s1/2) states in the Ic, IIabc intermediate states, as they are not ruled out by the Gell-Mann denominator. In the J=1 case the II portion plays a more significant role than in the J=0 case.

Based on this table we may get an idea of the importance of the classes of intermediate states left out. The suppression of IIc relative to Iab is mainly due to energy denominators. The dangling diagrams omitted in chapter 5 will be suppressed even further by this effect.

We now repeat the earlier calculation of W Iab including massive quarks, with a particular emphasis on obtaining an idea of the convergence of the sum.

Table 6.7 shows a calculation of W Iab for two quarks coupled to J=0. We show the result for various kappa values of the intermediate quarks. Quark pairs are forced to have the same kappa by angular momentum and parity considerations. The gluon J sum is finite, also from angular momentum considerations, as is the sum over gluon polarizations. The sum is truncated at gluon and quark radial quantum numbers equal to M. Each successive column shows the difference caused by incrementing M.

It can be seen from the table that the sum over radial quantum numbers converges reasonably quickly, although the number of terms increases as the fourth power of M. The sum over kappa is slower but still satisfactory. It is clear from the table that if we were to truncate the sum at M=2, and sum all kappa from -7 to 3 we would be making an error not larger than 1%.

This is therefore our guideline for a final sum of the series. (It includes contributions not shown in Table 6.6.) Table 6.7 shows the consolidated results for quark pairs of varying masses. The task of repeating this calulation for different masses is rather difficult, because the entire calculation right from the quark eigenenergy table to the radial overlap integrals has to be repeated.

Table 6.7 : Summary of W

Intermediate quark kappa : -7..3; gluon J=0..7; M=2.
Initial state : Two 1s1/2 states coupled to J.

Mass : a - 0.0
b - 1.5
c - 1.85

	I - J=0	II - J=0	I - J=1	II - J=1
Maa	-0.764051	-0.050108	-0.225751	-0.079318
Mab	-0.697577	-0.070115	-0.251577	-0.068106
Mbb	-0.686977	-0.091493	-0.288073	-0.064374
Mac	-0.684347	-0.074721	-0.258088	-0.066847
Mcc	-0.684134	-0.101097	-0.307202	-0.065537

For convenience we include the 2nd order results.

	J=0	J=1
Maa	0.5408	-0.1670
Mac	0.4224	-0.1069
Mcc	0.3667	-0.0335

6.2 Two Gluon Annihilation

In this section we describe the practical evaluation of the expression for two gluon annihilation. There are essentially two contributions arising from what we refer to as straight and crossed diagrams as shown in Figure 6.1.

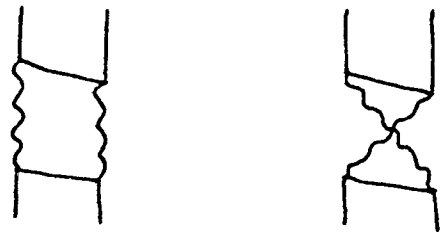

'straight' 'crossed'

Figure 6.1 : Two gluon annihilation

The sum of these two diagrams is required to symmetrize the intermediate two gluon state.

In the same way as the previous section we split up and calculate the colour, angular momentum and radial contributions, and recombine as appropriate. Once again the colour contribution simplifies. From the completeness and trace orthogonality of the traceless Hermitian SU(N) generators $M^k_{c'c}$, k=1..N^2-1, given that

$$Tr\ M^k M^l = \delta_{kl}\ S \tag{6.23}$$

It can be shown that

$$\delta_{c'd'}\,\delta_{cd} = {}^1/_N\ \delta_{c'c}\,\delta_{d'd} + {}^1/_S\ M^k_{c'c}\,M^k_{d'd} \tag{6.24}$$

This yields a useful relationship

$$(\lambda^a/2)_{c'd'}\,(\lambda^a/2)_{dc} = 4/9\ \delta_{d'd}\,\delta_{c'c} + (\lambda^a/2)_{c'c}\,(-\lambda^a/2)_{dd'} \tag{6.25}$$

The left hand side is the colour factor for $q\bar{q}$ annihilation via a single gluon, and this expression enables one to express the fact that only colour octets can annihilate, in terms of the colour dot product. In the case of two gluon annihilation we have

$$(\lambda^a/2)_{c_1 c_5} (\lambda^b/2)_{c_5 c_2} (\lambda^d/2)_{c_4 c_6} (\lambda^c/2)_{c_4 c_6} \; a^+_{c_1} \; b^+_{c_2} \; b_{c_4} \; a_{c_3} \tag{6.26}$$

multiplied by $\delta_{ac}\delta_{bd}$ for straight and $\delta_{ad}\delta_{bc}$ for crossed graphs. Using the above identities one may reduce the straight and crossed graphs respectively to

$$3 \; 4^2/9^2 \; - \; 1/18 \; \vec{\lambda}_1/2^Q \cdot \vec{\lambda}_2/2^{\bar{Q}} \tag{6.27}$$

$$-2/27 \; - \; 5/9 \; \vec{\lambda}_1/2^Q \cdot \vec{\lambda}_2/2^{\bar{Q}} \tag{6.28}$$

These results were checked by computer and are displayed in Table 6.4. Two gluons combined to a colour singlet are symmetric under permutation, therefore the colour contributions for singlet qq must be equal for straight and crossed graphs. Two gluons in a colour octet can be in a symmetric or antisymmetric state, so this argument does not apply.

The 1- mesons cannot decay into two gluons. We recall the familiar case of Parapositronium, which cannot decay into two photons. There are at least two distinct reasons for this.

Photons are bosons, and physical photons must be transverse. In the rest frame of a particle that decays into two photons they must possess zero total momentum. Table 6.8 lists the multiplicities of such two photon systems for various possible parities P, and total angular momenta J, of some decaying particle (Be 82).

Table 6.8 : Two photon decay

J	P=+	P=-
0	1	1
1	0	0
2n	2	1
2n+1	1	0

Another line of argument relies on charge parity. The photon has negative C-parity, whereas the C-parity of positronium is

$$C = (-)^{L+S} \tag{6.29}$$

Therefore ground state parapositronium is excluded from decay into an even number of photons (Furry's theorem).

In the case of confined gluons the first argument does not apply. The gluons are intermediate states and need not be physical, i.e. transverse. In the bag model they will not possess good total momentum. Also, the confinement boundary conditions introduce a distinction between magnetic and electric gluons by giving them different discrete spectra. Thus when we combine 1M1 and 1E1 gluons to zero angular momentum it is impossible to get their total momentum to be zero in the rest frame of the bag. This may be seen by following the argument that leads to Table 6.8.

Clearly Furry's theorem does not apply either. However we can examine the implications of charge conjugation in QCD. Consider an SU(3) transformation (de 63) on an object with triplet charge $\{3\}$.

$$x'_c = U_{cd}\, x_d \qquad c,d = 1,2,3 \tag{6.30}$$

The contragredient representation $\{\bar{3}\}$ transforms according to

$$y'_c = U^*_{cd}\, y_d \tag{6.31}$$

and clearly

$$U^* = (U^{-1})^T \tag{6.32}$$

However

$$U = \exp\{ i \vec{\alpha} . \vec{\lambda}/2 \} \tag{6.33}$$

Thus the generators for the contragredient representation are

$$-\lambda^*/2 = -\lambda^T/2 \tag{6.34}$$

We expect our Lagrangian to be invariant under this operation, which suggests that

$$\vec{A} \rightarrow -\vec{A}^* \tag{6.35}$$

Representations D(p,q) are contragredient to themselves if p=q. The (Y=0, M_T=0) member will be an eigenstate of the charge conjugation operation.

In the colour (Y, M_T) plane charge conjugation is equivalent to inversion. This is because the ladder operators (Y, I_3) go to ($-Y, -I_3$) under .

When two colour octet gluons are combined to a singlet, each octet basis element is combined with equal weight to its inverted partner. The colour labels are symmetric under permutation, as must be the rest of the wavefunction. Charge conjugation will be equivalent to swopping colour labels, therefore the charge parity of the two gluon system is positive.

In the case of mesons in the bag model, the qq wavefunction must be antisymmetric. The permutation operator consists of a permutation in colour-isospin, orbitals and angular momentum. Therefore

$$-1 = P_{CT} P_J P_O \tag{6.36}$$

In our case both quark and antiquark are in 1s1/2 states, and

$$P_J = (-)^{J+1} \quad \text{ie} \quad P_{CT} = (-)^J \tag{6.37}$$

So $q\bar{q}$ combined to 0- (1-) has + (-) C-parity. This provides the prohibition on the 1- decaying into two gluons.

Table 6.9 presents the results for two gluon annihilation, for $q\bar{q}$ coupled to 0-. Both intermediate gluons must have the same angular momentum J, different polarization (to get negative parity), and may or may not have different radial quantum numbers. We treat each J value seperately. For each J, the sum over kappa of the intermediate quark is cut of by angular momentum considerations. What remains is the sum over radial quantum numbers of all quarks and gluons, and gluon polarizations. We truncate the sum over radial quantum numbers (quarks and gluons) at some M.

The first column shows the results for M=1, the next column shows the additional contribution when M=2. Clearly there are many ways of combining the different radial quantum numbers. The number of terms in this sum goes as the 4th power of M. Because of the decrease in the radial overlap integrals, these terms contribute little. The convergence of the sum as J increases is more slow, but is still satisfactory.

The dominantly contributing intermediate gluon pairs are (1M1,1S1) and (1M1,1L1). They contribute 0.79 and -.52 respectively, summing to 0.27. As mentioned previously, the scalar gluon raises the unperturbed energy, and the longitudinal gluon lowers it. The cavity energy eigenvalue of each pair is

$$2.744\ (1M1) + 2.082\ (1S1) = 4.826 \tag{6.38}$$

This differs from the initial qq state by the relatively small amount of 0.74. Before looking at the magnitude of this result, the sign warrants comment. If we assume that the η and η' are split upwards from the π by mixing with a two gluon state that has higher energy eigenvalue, then we are forced to concede that it must dominantly contain a single scalar gluon. In other words, the correct sign of our result is non-trivial.

These results were obtained independently of (Do 83) who performed their calculation in the Coulomb gauge. Their result is 0.39 as opposed to 0.29, which could be attributed to our omission of some of the intermediate states. We have not performed the calculation as a function of mass, because the energy gap decreases and there are large subtraction errors. It is not absolutely clear whether perturbation theory applies here, and non perturbative treatments will require application of the subsidiary condition.

Table 6.9 : Two gluon annihilation

Initial state : Two 1s1/2 quarks coupled to 0-
Intermediate state : Two gluons, angular momentum J

All possible intermediate quark kappa's, and gluon polarizations are summed, the intermediate gluon and quark radial sum is truncated at M. The colour and angular momentum factors are included. To obtain the energy shift multiply by α^2/R.

J	M=1	M=2	M=3
1	0.250836	-0.006248	-0.000290
2	0.034722	-0.000770	-0.000158
3	0.009786		
4	0.003810		
5	0.001792		

TOTAL = 0.294 +/- .002

7 COEFFICIENTS OF FRACTIONAL PARENTAGE

7.1 Notation

Thus far we have calculated 2nd and 4th order perturbative energy shifts for qq and $q\bar{q}$ state vectors in arbitrary colour representations. We would now like to calculate the corresponding shifts in three quark systems. We might also wish to calculate energy shifts for systems such as a hypothetical six quark bag.

In the process of evaluating the 2nd and 4th order perturbative energy shifts in section 5 we arrived at an effective two body operator. The energy shift for two quark states is the expectation value of this operator.

We should note that in calculating the diagrams in section 5, some of the intermediate states are not antisymmetrized. Only with the inclusion of the self energy diagrams (and the three body operator, in the case of baryons) would we get fully antisymmetrized wavefunctions at all steps of the calculation.

In order to investigate three quark systems we must firstly know the fully antisymmetrized wavefunction. Ideally the next step would be to calculate the three quark 4th order energy shift operator and add this to the two quark operator already calculated. We have not calculated this three body operator.

In order to calculate matrix elements of two body operators in three quark systems we introduce the notation of coefficients of fractional parentage. This formalism enables us to easily handle two body operators in N body antisymmetrized systems.

Our N quark fully antisymmetrized wavefunction may in general be written

$$\Phi^{N}_{S K K_P} \qquad (7.1)$$

s refers to the multiplicity, and simply enables us to distinguish between different states with the identical quantum numbers. These states generally differ in the way that they are constructed to be fully antisymmetric. In other words they are multiple eigenstates of all the permutation operators Pij with eigenvalue equal to -1. The operator Pij permutes all labels of particles i and j in the wavefunction.

k and κ respectively contain the principal and magnetic quantum numbers for colour, isospin and angular momentum i.e. k=(F^2, G^3, T^2, J^2); κ =(T^c, T_z^c, Y^c, T_z, J_z). We use the notation of (de 63) for the colour quantum numbers.

p denotes the number of quarks in each shell. The parity is implicit in p.

What we in fact wish to calculate are matrix elements of the form

$$X = \langle {}_1\Phi^N \left| \sum_{1\le i<j\le N} \Delta(i,j) \right| {}_2\Phi^N \rangle \qquad (7.2)$$

where $\Delta(i,j)$ is some two body operator. The subscript distinguishes between potentially different wavefunctions. We can immediately see that for ${}_1\Phi^N, {}_2\Phi^N$ (anti)symmetric the above expression reduces to

$$X = \tfrac{1}{2} N(N-1) \langle {}_1\phi^N \left| \Delta(1,2) \right| {}_2\phi^N \rangle \qquad (7.3)$$

In other words we only really need to know the two body content of the wavefunctions in order to evaluate X.

Each Φ^N may be expressed as a sum of direct products of fully antisymmetrized wavefunctions refering to the first 2 particles, and the remaining N-2.

$$\Phi^N_{s\,k\,K\,p} = \sum_{s_1 k_1 p_1\, s_2 k_2 p_2} C^{N\,s\,k\,p}_{2\;s_1 k_1 p_1\; s_2 k_2 p_2} \sum_{K_1+K_2=K} (k_1\, K_1\; k_2\, K_2 \mid k\, K)\, \Phi^2_{s_1 k_1 K_1 p_1}\, \Phi^{N-2}_{s_2 k_2 K_2 p_2} \qquad (7.4)$$

where $C^N_{2,N-2}$ are the coefficients of fractional parentage of the two body wavefunction embedded in the N body wavefunction, and $(k_1 K_1 k_2 K_2 \mid k, K)$ are the Clebsh Gordan coefficients in the colour, isospin and angular momentum spaces. The SU(3) Clebsch Gordans may be found in (de 63).

Now in order to evaluate the $\Delta(1,2)$ matrix element between N body states, we briefly expand both sides according to (7.4). We then exploit the orthogonality of the N-2 body wavefunctions.

Our two body matrix elements will be of the form

$$\langle \phi^2_{s_1 k_1 p_1} \mid \Delta(1,2) \mid \phi^2_{s_2 k_2 p_2} \rangle \qquad (7.5)$$

Our interactions conserve colour, and angular momentum. When we deal only with u and d quarks, we may regard isospin as a conserved quantum number. When we include the s quark our interactions do not respect flavour independence, and we should not seperate flavour and orbital-angular momentum spaces.

We proceed with the calulation in the case that the interaction is isospin independent. The matrix elements will be diagonal in k and will have no dependence on K. It is also diagonal in s, because in a two body system the multiplicity is always one. (The system can only be symmetric or antisymmetric.)

This enables us to take the two body matrix element out of the sum over K_1, K_2 and exploit the orthogonality of the generalized Clebsch Gordans

$$\sum_{K_1 K_2} (k_1 K_1 k_2 K_2 \mid k K)(k_1 K_1 k_2 K_2 \mid k' K') = \delta_{k k'}\, \delta_{K K'} \qquad (7.6)$$

The result, omitting labels is

$$\langle \phi^N_{s_1 k_1 p_1} | \Delta(1,2) | \phi^N_{s_2 k_2 p_2} \rangle$$
$$= \sum_{s_3 k_3 p_3 \, s_5 k_5 p_5 \, p_4} C^{N s_1 k_1 p_1 *}_{2 s_3 k_3 p_3, N-2 s_5 k_5 p_5} C^{N s_2 k_2 p_2}_{2 s_3 k_3 p_3, N-2 s_5 k_5 p_5}$$
$$\langle \phi^2_{s_3 k_3 p_3} | \Delta(1,2) | \phi^2_{s_3 k_3 p_4} \rangle \qquad (7.7)$$

7.2 Calculation

We outline the method for the isospin independent case, the flavour dependent case is a straightforward extension of the method.

A basis wavefunction can be constructed out of direct products of wavefunctions in colour, isospin and orbital-angular momentum spaces. (Once one goes beyond the p1/2 and s1/2 shells the orbital and angular momentum may not be written as a direct product.) Although in the end we only use a few of the results, we have written computer code that will solve the three body problem in general. The results would be useful for a calculation of the static properties of hadrons with significant admixtures of other states. We outline the method.

In each of the three spaces we set up a basis of symmetric and antisymmetric two body wavefunctions coupled to good colour, isospin or angular momentum. As a rule we always adhere to the Condon Shortley phase convention for Clebsch Gordan coefficients (and their SU(3) generalization (de 63)). This leads to

$$| s_{1/2} \; p_{3/2} \; J=1 \rangle + | p_{3/2} \; s_{1/2} \; J=1 \rangle \qquad (7.8)$$

being overall antisymmetric under permutation of particle 1 and 2.

In each space we now add a third quark and form a basis of all possible three body states, again with good quantum numbers. Many of these states will now have mixed symmetry.

Now we group together states with the same principal quantum number, and evaluate the matrix elements of the P23 operator in each space. For example in pure SU(2) isospin the results are trivial

$$P_{23}\,|3/2\rangle = |3/2\rangle$$

$$P_{23}\,|1/2\rangle_S = -1/2\,|1/2\rangle_S + \sqrt{3}/2\,|1/2\rangle_A$$

$$P_{23}\,|1/2\rangle_A = \sqrt{3}/2\,|1/2\rangle_S + 1/2\,|1/2\rangle_A \qquad (7.9)$$

The kets represent three isospin 1/2 particles coupled together to isospin $|T\rangle$ and the subscript denotes the P12 symmetry for the mixed symmetry T=1/2 cases.

For SU(3) colour we need only consider three quarks coupled together to $\{1\}$, which is completely antisymmetric. For the orbital-angular momentum space the task is non-trivial and a computer program is used.

The next step is to form direct product wavefunctions corresponding to some choice of principal quantum numbers. Using

$$P_{ij} = P_{ij}^{C}\; P_{ij}^{T}\; P_{ij}^{O-J} \qquad (7.10)$$

We compute P12 for each wavefunction and discard those with P12=+1. Then we compute the matrix of P23 on the remaining wavefunctions. On diagonalizing the matrix, those wavefunctions with eigenvalue -1 correspond to fully antisymmetrized three body states. The numbers in the eigenvector correspond to the coefficients of fractional parentage as defined by (7.4).

Table 7.1 shows the coefficients of fractional parentage for some nucleon and delta states. The lowest $(1s1/2)^3$ and next lowest $(1s1/2)(1p3/2)^2$ three quark states with the quantum numbers of the nucleon and delta are tabulated. The nucleon $(1s1/2)(1p3/2)^2$ state is doubly degenerate.

The coefficients of fractional parentage are shown next to the corresponding antisymmetrized two body content. It is to be understood that the square root of all the coefficients should be taken, and the sign indicates the sign of the square root. The remaining one body content will be a $\{3\}$ T=1/2 1s1/2 or 1p3/2 as appropriate.

In Table 7.2 we show the coefficients of fractional parentage for the decuplet and octet, where the flavour breaking forces us to combine flavour with the orbital-angular momentum space. All quarks are in the lowest orbital.

Table 7.1 : Coefficients of Fractional Parentage

A=1s1/2
B=1p3/2

Cfp	COLOUR	ISOSPIN	Orbital-J
Nucleon	{1}	T=0.5	AAA J=0.5
1/2	{3}	T=0.0	AA J=0.0
1/2	{3}	T=1.0	AA J=1.0
Nucleon	{1}	T=0.5	ABB J=0.5
1/16	{3}	T=0.0	AB J=1.0
1/3	{3}	T=0.0	BB J=0.0
-5/48	{3}	T=0.0	AB J=2.0
-3/16	{3}	T=1.0	AB J=1.0
5/16	{3}	T=1.0	AB J=2.0
0	{3}	T=1.0	BB J=1.0
Nucleon	{1}	T=0.5	ABB J=0.5
-5/16	{3}	T=0.0	AB J=1.0
0	{3}	T=0.0	BB J=0.0
-3/16	{3}	T=0.0	AB J=2.0
-5/48	{3}	T=1.0	AB J=1.0
-1/16	{3}	T=1.0	AB J=2.0
-1/3	{3}	T=1.0	BB J=1.0
Delta	{1}	T=1.5	AAA J=1.5
1	{3}	T=1.0	AA J=1.0
Delta	{1}	T=1.5	ABB J=1.5
-1/2	{3}	T=1.0	AB J=2.0
-1/3	{3}	T=1.0	BB J=1.0
1/6	{3}	T=1.0	AB J=1.0

Table 7.2 : Coefficients of Fractional Parentage

A=1s1/2
B=1p3/2

All quarks in 1s1/2 states.
Only the most positively charged member of each isospin multiplet shown.

Decuplet Hadrons

Cfp	Colour	Flavour	J
	1	uuu	1.5
1	3	uu	1.0
	1	uus	1.5
2/3	3	us	1.0
1/3	3	uu	1.0
	1	uss	1.5
2/3	3	us	1.0
1/3	3	ss	1.0
	1	sss	1.5
1	3	ss	1.0

Octet Hadrons

Cfp	Colour	Flavour	J
	1	udu	0.5
-1/2	3	ud	0.0
-1/3	3	uu	1.0
1/6	3	ud	1.0
	1	usu	0.5
1/6	3	us	1.0
-1/2	3	us	1.0
-1/3	3	uu	1.0
	1	dsu	0.5
1/12	3	ds	1.0
-1/4	3	ds	0.0
0	3	ud	0.0
1/12	3	us	1.0
-1/4	3	us	0.0
-1/3	3	ud	1.0
	1	dsu	0.5
1/4	3	ds	1.0
1/12	3	ds	0.0
-1/3	3	ud	0.0
-1/4	3	us	1.0
-1/12	3	us	0.0
0	3	ud	1.0
	1	uss	0.5
1/6	3	us	1.0
-1/3	3	ss	1.0
1/2	3	us	0.0

8 TWO BODY INTERACTIONS AND BARYON SPECTRA

In this section we present the two body interactions and the resulting baryon spectra in the framework of the MIT bag model. Although based on the detailed results of sections 5, 6 and 7, this section may be read independently as a survey of the pertinent results, provided one reads the introductory parts of section 5. But first we try to give an understanding of the accuracy of the perturbative method.

8.1 Accuracy

In section 6 we discussed the validity of perturbation theory. In particular we looked at the extent of the admixtures of intermediate states. Before proceeding with plots of the perturbative energy shifts, we would like some kind of estimate of the error in the energy predicted by perturbation theory.

We firstly consider the second order hyperfine interaction. In Figure 8.1 we show the splitting in energy as a function of α_s for a $q\bar{q}$ pair, both in 1s1/2 states, coupled to J=0 and J=1, and in a colour $\{1\}$. These states correspond to the π and ρ mesons. The (cavity) energy is in units of 1/R. The dominant part of the second order interaction is due to the exchange of a 1M1 gluon. The straight lines show the effect of this perturbative shift.

To gain insight into the error in the energy we construct a truncated space model. We diagonalize the Hamiltonian in the space of the $q\bar{q}$ state and the $q\bar{q}g$ (g=1M1) state. (The energy eigenvalues will in general be pushed apart, so we put $q\bar{q}g$ below $q\bar{q}$ for rho to get the right sign for the splitting.) This two level system is exactly solvable. We then plot the result for the energy shift, and compare the results. At low α_s the two curves coincide as expected. The discrepancy increases with α_s.

This provides us with an estimate of the error, but may in no way be considered an exact, or more exact, calculation. Only with inclusion of the self energy, necessitating renormalization, could we consider diagonalization exact, even in a truncated space.

This error could be thought of as due to the effect of a specific subclass of higher order perturbative corrections, specifically those gained by repeating the process under consideration in a ladder.

Figure 8.1 shows that the error is significant for $\alpha_s \simeq 1$ for the π. Although significant, the trend is largely unchanged, even up to the region we will finally be interested in, namely $\alpha_s \simeq 1.5$.

Figure 8.2 shows a similar calculation for the 4th order perturbation of the same two states. The lower curves for the π and ρ show the 2nd order plus 4th order perturbative energy shifts. In the 4th order contribution only the (dominant) contribution from intermediate $(1p3/2)^2$ states is included. This enables us to recalculate the upper curves, based on a two level model containing the $(1s1/2)^2$ and $(1p3/2)^2$ qq states, and an effective Hamiltonian for one gluon exchange. We see that for the ρ the agreement is excellent, even up to $\alpha_s \simeq 2$. However for the π the perturbation theory result significantly overestimates the energy shift.

8.2 The Two Body Interactions

We now examine the two body interactions of two massless quarks in the lowest cavity eigenmodes, based on the results presented in section 6. We are interested in the 2nd plus 4th order perturbed energy as a function of α_s. The 2nd order shifts are given explicitly in section 5, and the 4th order shifts in section 6.

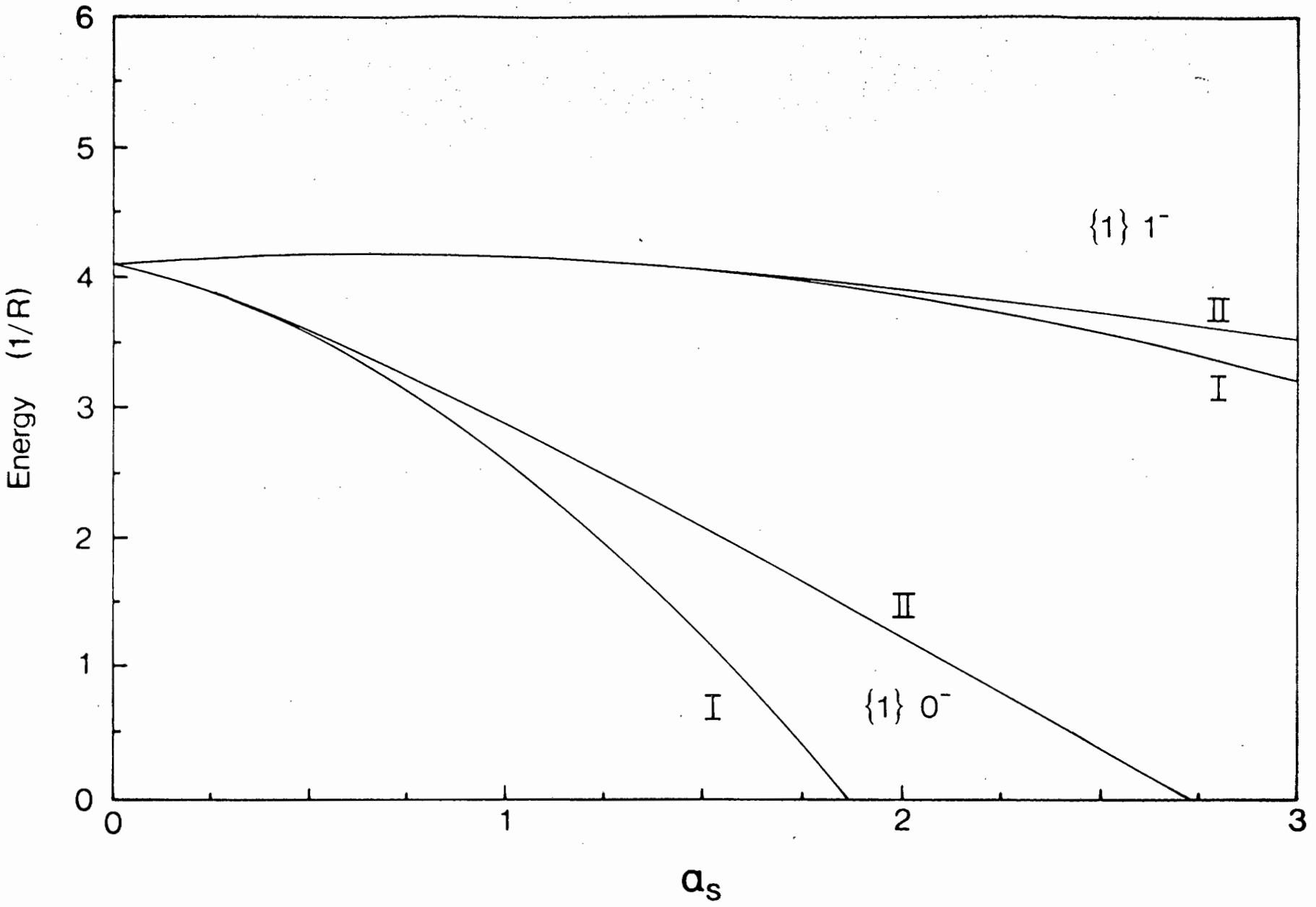

Figure 6.2 : Rho-pi splitting I - 2nd + 4th Order Perturbation theory
II - Two level model

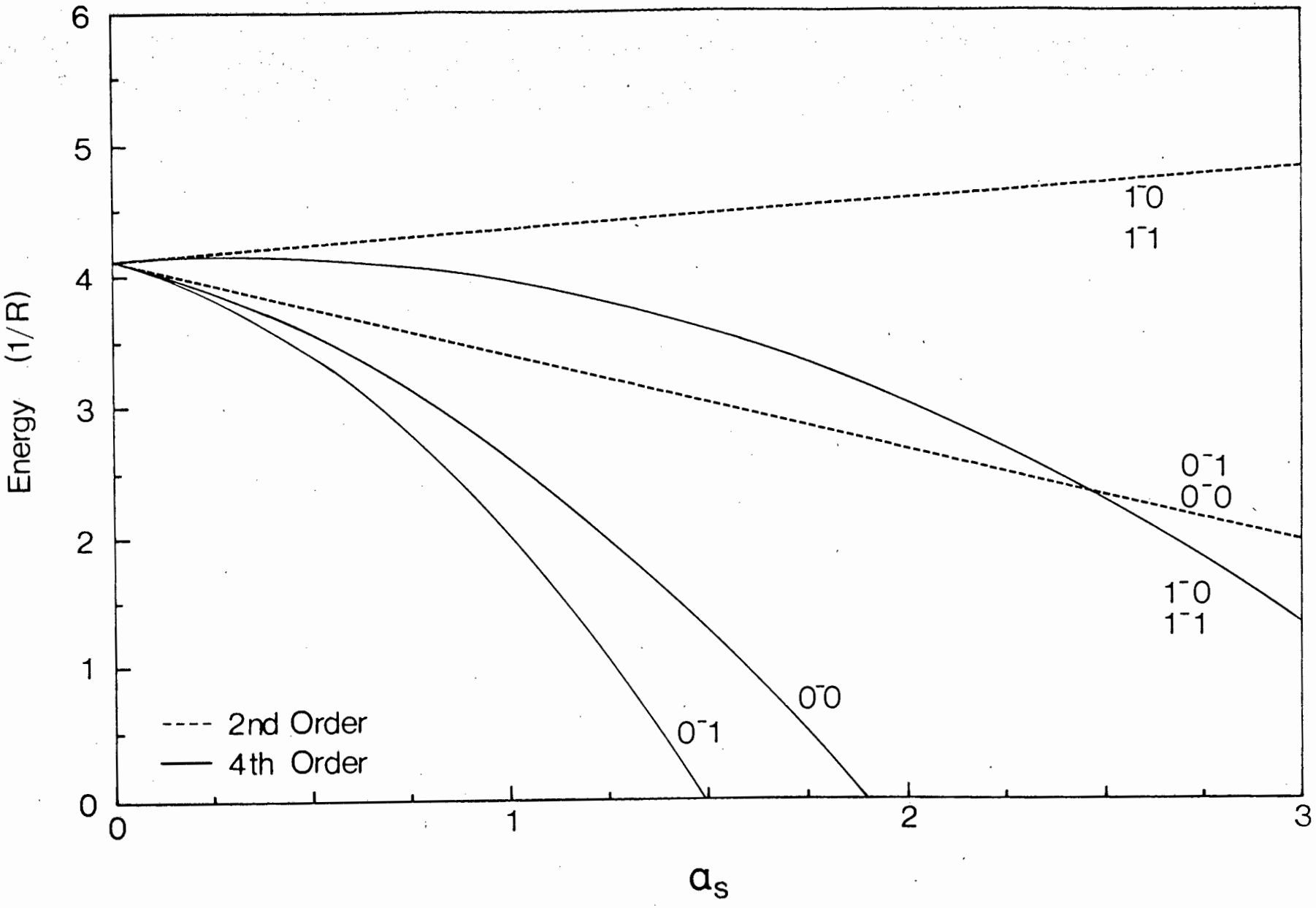

Figure 6.3 : (1) 2nd & 2nd+4th perturbation Curves labelled by J^PT

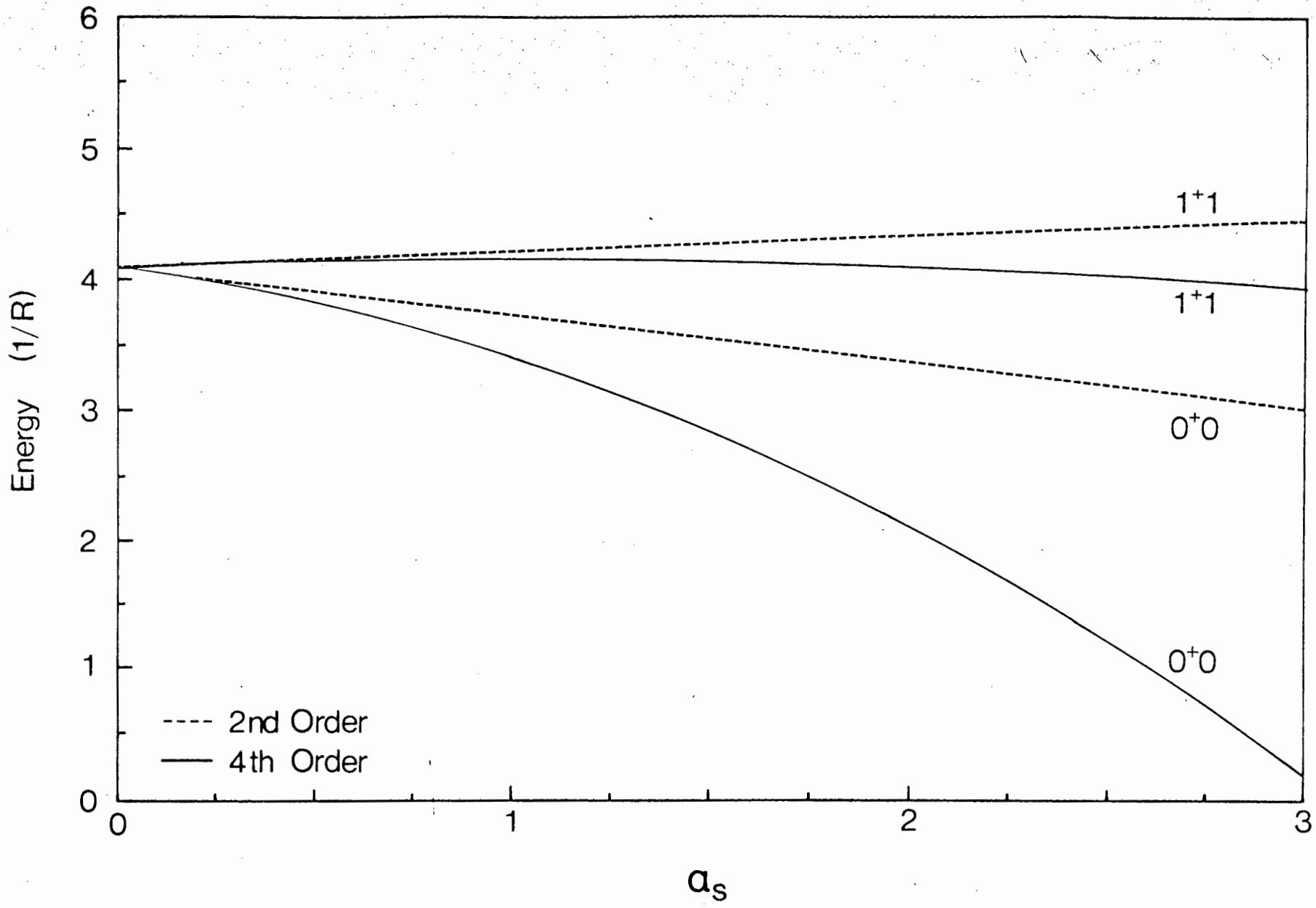

Figure 6.4 : $\{\bar{3}\}$ 2nd & 2nd+4th perturbation Curves labelled by $J^P T$

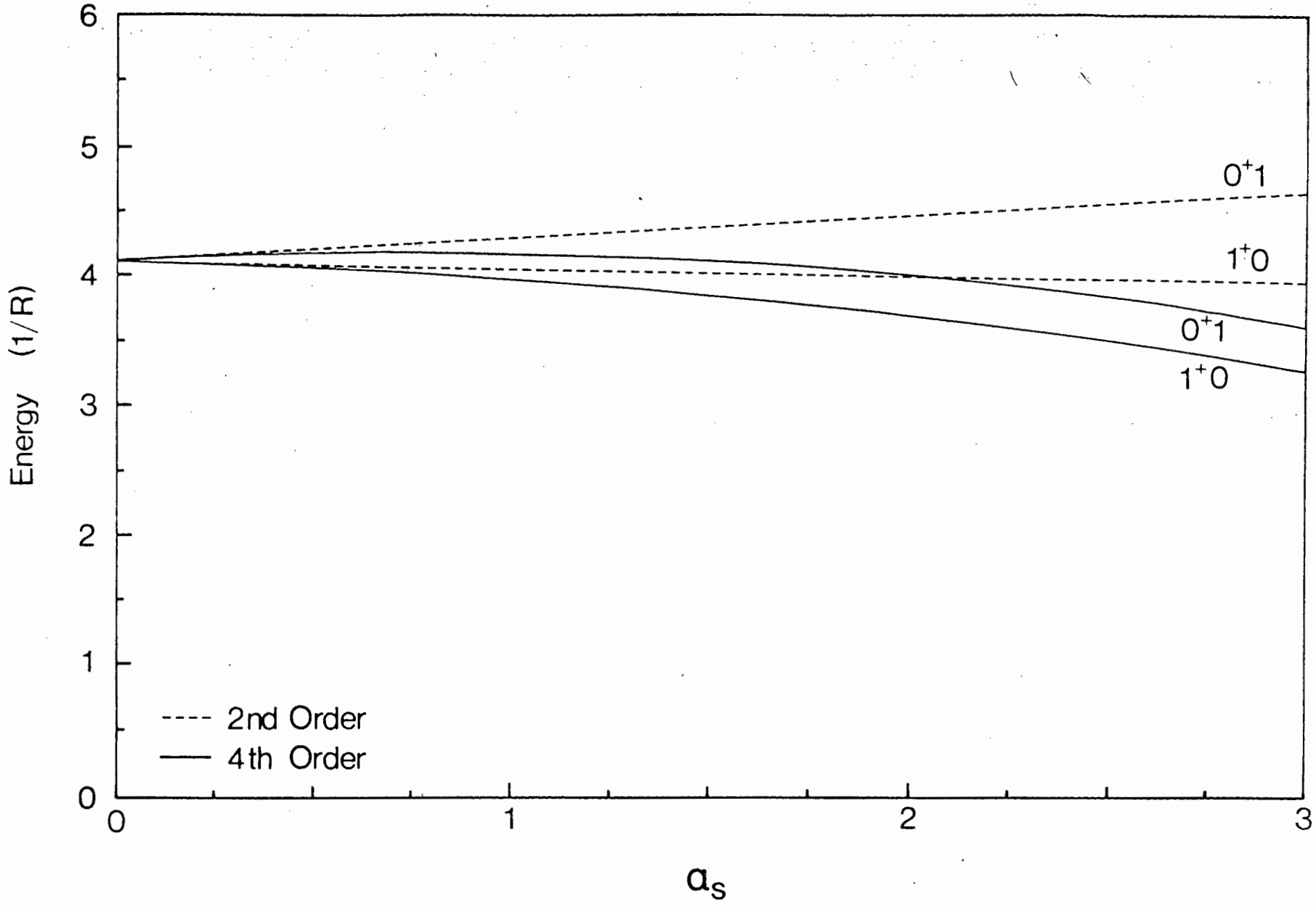

Figure 6.5 : {6} 2nd & 2nd+4th perturbation Curves labelled by $J^\pi T$

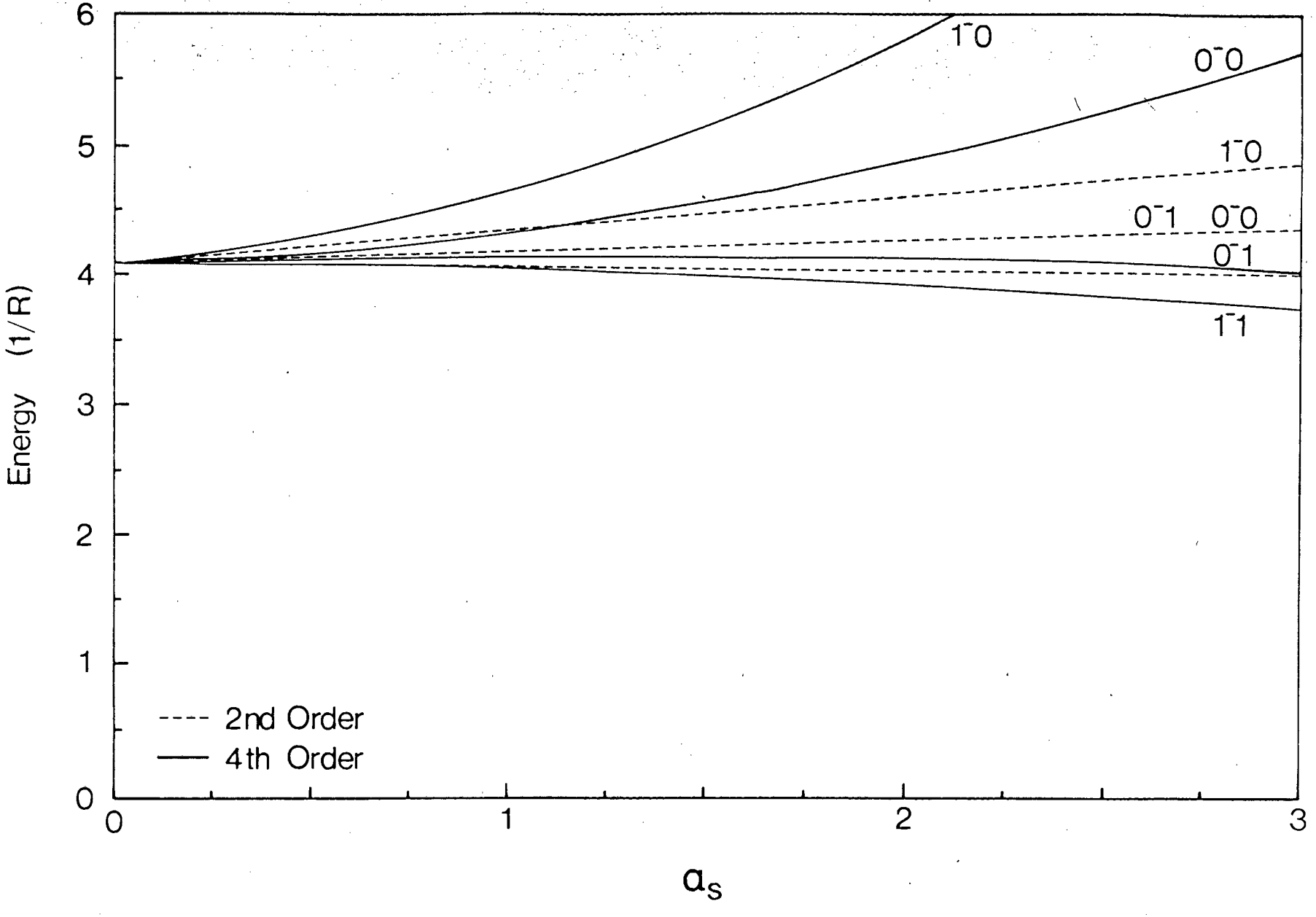

Figure 6.6 : {8} 2nd & 2nd+4th perturbation Curves labelled by $J^P T$

Two quarks, or an antiquark-quark system can combine to four different SU(3) colour representations, namely the colour singlet and octet ($q\bar{q}$), and triplet and sextet (qq). Only the colour singlet and triplet are relevant for (colour singlet) mesons and baryons. However, the other interactions are important insofar as they appear in exotic states. In order to be consistent with experiment the theory must not predict any such states where they are not observed, thus any strongly attractive channels would be a disturbing signal.

Figures 8.3 to 8.6 show the two body interactions. The two body systems can combine to J=0 or J=1. The isospin of the fermionic qq systems is immediately fixed by the requirement of antisymmetry. In the qq systems isospin T=0 or T=1 is possible. These two states will be degenerate under one gluon exchange, but one and two gluon annihilation processes, which only affect T=0 states, will lift this degeneracy.

The straight (dotted) lines in Figures 8.3 to 8.6 show the second order perturbative energy shifts. The colour octet includes the one gluon annihilation shift as given in (Zi 86). In fact, this process plays the dominant role in the octet 2nd order shifts. The parabolas show the 2nd plus 4th order results.

The sextet interactions remain weak in comparison to the other channels, as do most of the octet channels except those that become significantly lifted by the two gluon annihilation process. Octet configuration mixing is strongly suppressed by the colour factors (see Table 6.4).

In the colour singlet and triplet channels we see the J=0 states strongly bound, and we know that particularly for the colour singlet, the perturbative result is a significant overestimate. In the colour singlet we see the isoscalar pseudoscalar channel split upwards from the pion. It is not split by quite as much as we would like in order to fit the eta, which is considerably heavier than the pion, but we know from the above discussion on

errors that higher order contributions raise both curves. (The splitting is a more reliable quantity.)

8.3 The MIT Bag Model

We would like to comment on the effects of these additional contributions to the two quark interaction in baryon spectra. There is no clear theoretical link between the cavity field theory and quark bound states. However, there have been many phenomenological models that attempt to make this connection. We do not wish to consider the effects that different models may have when combined with our results. We simply use the standard MIT bag model (Ch 74, De 75), which historically provided the motivation for attempts to formulate the field theory in a cavity.

A full discussion of the MIT bag model is beyond the scope of this thesis, so we will simply motivate the terms that constitute the baryon mass in this model. Our intention is to calculate the baryon spectrum in the MIT bag model, incorporating the 4th order contribution.

In the model the empty bag has a energy proportional to the volume. This is supposed to account for the energy necessary to 'melt' the vacuum. In terms of the bag constant B the energy is

$$E_B = BV = 4/3\,\pi\, B\, R^3 \qquad (8.1)$$

The so-called zero point term is included to account for the zero point or Casimir energy associated with the empty cavity. It could also account for other effects, such as center of mass corrections or the self energy. Although in principle these effects are all calculable in reality Z_0 simply functions as an additional parameter, without which it would be difficult to get a good fit. The zero point term is

$$E_Z = -Z_0/R \qquad (8.2)$$

The energy of the unperturbed quark cavity modes is given by a term of the form

$$E_q = \sum_i \omega_i(m_i)/R \tag{8.3}$$

The perturbative corrections of section 5 contribute to the total energy terms, linear and quadratic in the strong coupling constant,

$$E_P = \sum_{i<j} V_{ij} + W_{ij} + U_{ij} \tag{8.4}$$

The original MIT bag paper included only the 2nd order contribution, in this calculation we now include some of the 4th order part. The total energy of the hadron will now be a function of the radius

$$E(R) = E_B + E_z + E_q + E_P \tag{8.5}$$

According to the model one should now minimize the energy with respect to the radius to get the actual mass of the baryon.

The radial dependence is of the form

$$E(R) = A/R + 4/3\,\pi B R^3 \tag{8.6}$$

where A is dependent on α_s and Z_0,

$$A = f(\alpha_s) - z_0 \tag{8.7}$$

It is easily shown that

$$\left(E_2/E_1\right)^{4/3} = A_2/A_1 \tag{8.8}$$

so given three masses, i.e. two ratios, we may solve for B , Z_0, and α_s .

8.4 The Hadron Spectrum in the MIT Bag model

We now repeat the procedure followed by the MIT group, incorporating the 4th order perturbation correction. The u and d masses are set to zero, as they are known to be very small from other experiments, and the model is not sensitive to this small value. We now have three parameters, B, Z_0, α_s which we use to fit some of the u,d sector of the spectrum, namely the N, Δ, and ρ. The s quark mass is varied to achieve a good fit to the Ω We defer a discussion of the isoscalar sector to section 8.5.

In the original MIT bag model a good fit (+/- 10%) was achieved for the decuplet and octet, and some of the pseudoscalar and vector nonets. The fit was poor for the pion. The pseudoscalar isoscalars were not fitted in this model, but a parameterization based on two gluon annihilation was offered.

Table 8.1 and Figure 8.7 show our results. The coupling constant is weaker than the original MIT model. This is easily understood from Figure 8.1 and 8.2, which show that the 4th order contribution increases the splitting between pairs of quarks coupled to J=0 and J=1. Most models subsequent to the MIT bag model have used smaller values of the coupling constant, for example (Ca 83, Fl 84) who correct for center of mass effects. These corrections are not yet of a rigorous nature. An (incomplete) study of the Coulomb spike effect (Ba 84) suggests that this effect alone may be responsible for decreasing α_s to a value consistent with heavy quarkonia non-relativistic potential models. This 4th order perturbation calculation takes the Coulomb spike into account to some extent.

The splitting between the Σ and Λ is very slightly improved in our fit. The radii are on the whole rather large, and this fact is connected with the Bag constant being somewhat smaller than the 146Mev of the MIT group. (Fl 84) suggest a $B^{1/4}$ of 230Mev, and argue that this is supported by other physics.

The fit is not significantly different to the MIT model, except in the behaviour of the pi. Our model predicts A to be negative for the pi, thus the minimum of E as a function of R occurs at R=0, i.e. the pion collapses against the (low) bag pressure. We can understand the reason for this by looking at Figure 8.3. The 4th order results dives down very rapidly as a function of α_s. The coefficient A=-0.19. If we add the error as read off Fig 8.1, namely +0.6/R, the new coefficient A=0.4. Using this value we get a mass for the pion of 172 Mev. This is not rigorous, but it suggests that we do understand the anomolous result for the pion.

8.5 The Isoscalars

In this section we try to estimate the mass of the η and η'. These mesons have always been a problem in the quark model. At first it seemed that, like the rho and omega, they should be degenerate. A possible explanation for their mixing, based on two gluon annihilation was given by (Is 76). This parameterized their splitting in terms of a process, which was in principle calculable.

There was subsequent confusion about the sign. A 'proof' (Ca 78) has appeared, showing that the term contributed by the two gluon process is of the wrong sign to explain the $\pi - \eta$ splitting. This point is discussed in section 6.4.

After a gap of 7 years, finally (Do 83) calculated the two gluon annihilation process in the Coulomb gauge. Their results are

$$\begin{aligned} \langle u\bar{u} \mid H_A \mid u\bar{u} \rangle &= 0.39\ \alpha^2/R \\ \langle u\bar{s} \mid H_A \mid u\bar{s} \rangle &= 0.29\ \alpha^2/R \\ \langle s\bar{s} \mid H_A \mid s\bar{s} \rangle &= 0.18\ \alpha^2/R \end{aligned} \qquad (8.9)$$

The experimental masses for the η and η' are 549 Mev and 958 Mev respectively. (Do 83), using a center of mass correction, are able to achieve a very good fit to these masses, 530 Mev and 965 Mev. They use one parameter $\alpha_s = 1.15$.

In our model it would be inconsistent to allow the freedom of this parameter which has already been fixed. We have not utilized center of mass corrections, as none of the existing techniques are of a rigorous, or nearly rigorous nature.

In the framework of the model of section 8.4, were we to attempt a prediction for the η , η', our predictions would clearly be only as good as our predictions for the pion and Kaon. For this reason we use these masses as input for a crude no parameter model of the η and η'.

As an estimate for the unshifted pseudoscalar uu+dd and ss energys we use the π and $2K - \pi$. This amounts to a crude assumption of linear dependence on strange quark mass. We then insert the two gluon annihilation process in a two level system. We could use the results of section 6.4, but we have not calculated the mass dependence, so we use (8.9). Thus our Hamiltonian looks like

$$\begin{bmatrix} E_\pi & \\ & 2E_K - E_\pi \end{bmatrix} + \alpha^2/R \begin{bmatrix} 0.78 & 0.41 \\ 0.41 & 0.18 \end{bmatrix} \qquad (8.10)$$

We use as input the value of α_s obtained from our previous fit, namely $\alpha_s = 1.38$, and the radius of the kaon. The results for the masses are 420 Mev and 995 Mev. Considering the crudity of the model, and the fact that no additional parameters have been introduced, the fit is quite satisfactory.

We note that the question of the quark content and mixing angles of the η and η' is still an open experimental question. There is still considerable model dependence involved in the interpretation of the experimental results, see for example (Ba 85).

Our results are considerably at odds with recent non-relativistic potential models (Fr 84, Fr 85). These models involve mixing with radial excitations and gluonia. They involve constituent masses, many parameters, and on the basis of this work, unreasonable assumptions. In particular they ignore orbital excitations like 1p3/2, which we see to mix more strongly (admittedly this is tied up with the use of constituent masses, and they in a non-relativistic sense have solved the center of mass problem). They ignore two gluon mixing of the kind that we find to be dominant. Instead they use gluonia which can only lower the mass. To their credit they fit more experimental results with their (many parameter) model, such as radiative decays.

Table 8.1 : Predictions for Baryon Spectra

Particle	m-exp(Mev)	m-bag(Mev)	R(fm)
Δ	1236	1236	1.19
Σ^*	1385	1387	1.24
Ξ^*	1533	1531	1.28
Ω^*	1672	1669	1.31
P	938	938	1.08
Λ	1116	1129	1.15
Σ	1189	1179	1.17
Ξ	1321	1331	1.22
ρ	770	770	1.01
ω	783	770	1.01
κ^*	892	939	1.08
ϕ	1019	1084	1.14
π	139	0	0
K	495	447	0.85

$B^{1/4}$=135.6 Mev $\quad \alpha_s$=1.386

Z_0=0.687 $\quad m_s$=1.85fm =364Mev

The underlined masses were used to fix the parameters

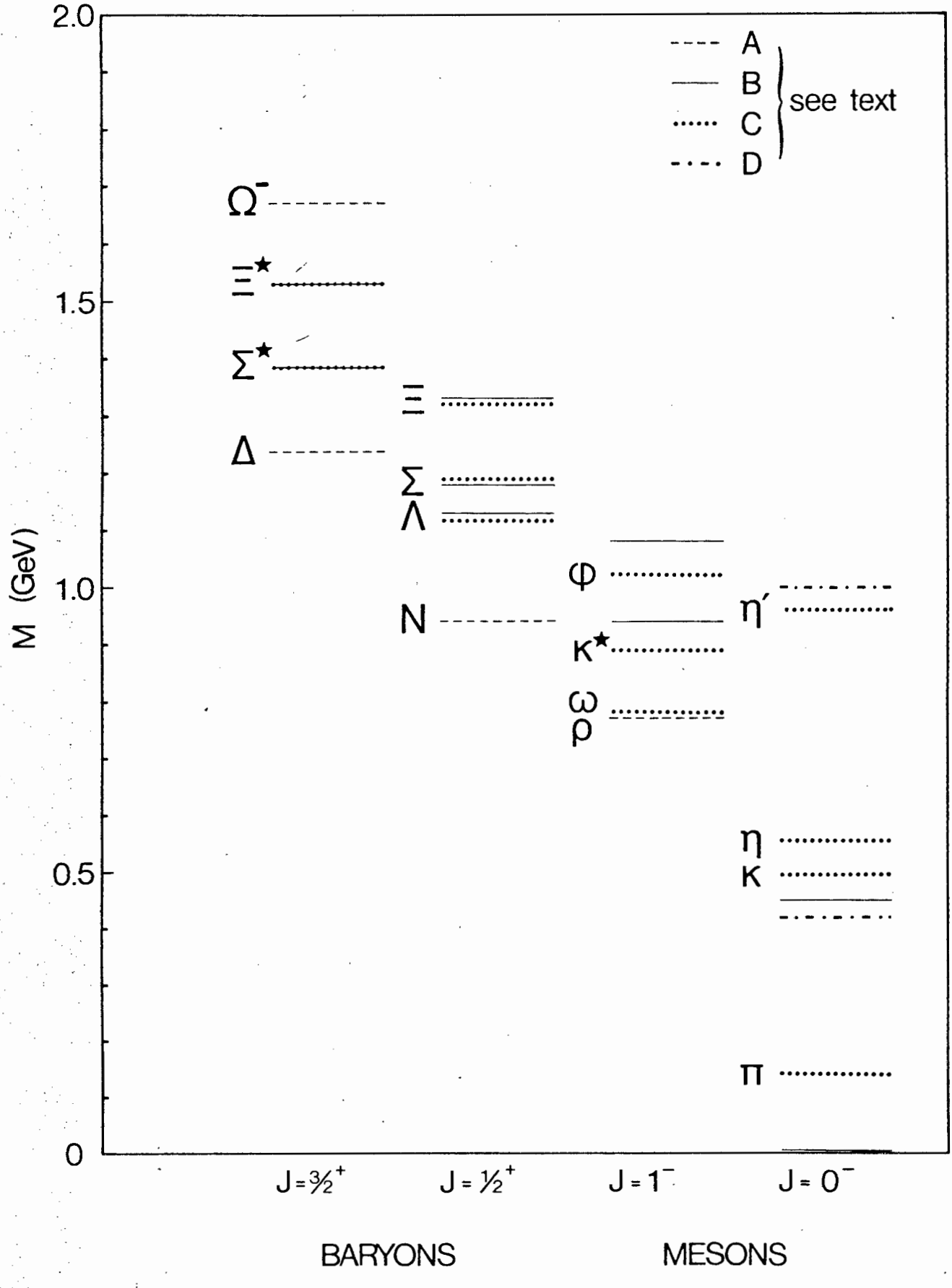

Figure 6.7 : Baryon Spectrum

A - Masses used to fix parameters
B - MIT + 4th order prediction
C - Experimental masses
D - Predictions of a simple model for the η, η' (see text).

9 CONCLUSION

The formalism of (Zi 86) has provided a solid base from which to investigate perturbative QCD in a cavity. We have formally calculated a subset of the 4th order diagrams, and obtained numerical results for the qq and $q\bar{q}$ systems in the lowest cavity mode.

The effect of the higher order diagrams is of course dependent on the value of α_s that one might prefer. For the range α_s from 1 to 2, which is the range of many models, the effect of the higher order diagrams is certainly significant, and perturbation theory is at or near its limits of validity.

It is encouraging that the higher order graphs increase the hyperfine splitting. This means that the value of α_s needed to fit a given splitting is smaller. However the ratio of pion shift to rho shift is less, implying that the hyperfine splitting will seem to determine the spectroscopy.

In the case of excited states, the effect of the higher order graphs is even more significant. Unless α_s is significantly smaller than 1, it may be that no reasonable explanation of excited states can be obtained without inclusion of the effects of configuration mixing

This is not as serious as it might seem, as non-perturbative truncated space models are easily implemented, once the processes have been calculated perturbatively. However these models will require that the divergences are properly dealt with.

The overall fit for the MIT bag is not significantly changed by the addition of the 4th order term, except for the pion, which is significantly lowered in energy.

For the first time a reasonable fit to the pseudoscalar isoscalars has been achieved without the use of additional parameters. It seems that any model that sets out to explain these particles must

take this Coulomb annihilation plus $q\bar{q}g$ mixing into account. Interest in this sector of particle physics is currently strong.

A serious and accurate description of the baryons based on QCD is still far away, but recent work (Ha 83, Do 83, Ba 85, Go 86, Zi 86) seems to indicate steady progress in cavity QCD.

At an immediate level there are many tasks that need to be carried forward. The 4th order diagrams tackled in this thesis can be exhaustively calculated. Using the coefficients of fractional parentage the effect of the perturbative corrections on the baryon static properties can be calculated. The strong admixtures suggest that there may well be significant effects on for example magnetic moments.

Now that the cavity self energy is available, this effect should be included in higher order calculations such as ours. Gluon self energies are of course a high priority, and will give a better prediction for glueball masses.

The calculation of (Ba 84) should be completed, extensions of this will enable the cavity picture to meaningfully tackle heavy quarkonia. This would be a not insignificant step, as we would then have a unified frameork, and may be able to gain insight from a comparison with the so-called relatavized potential models of light mesons (Go 85).

The center of mass problem remains a serious obstacle to cavity descriptions.

A subsidiary aim of this work was to gain an understanding of the prospects for the practical calculation of higher order diagrams in cavity QCD. There has been a protracted delay in the calculation of higher order diagrams since the original MIT bag model. In part this is due to the shaky foundations of the model, but is probably mainly due to the calculational complexity. The most interesting higher order diagram is certainly the two gluon annihilation, mentioned in many papers since 1976. The actual bag

model calculation occurred only in 1983 (Do 83), (and is not often cited, particularly by the potential model pundits (Fr 85).

Our formalism is compact, and essentialy shifts the labour of the calculation to the radial and angular factors of Appendix A. Both factors are then more easily handled by computer, even though both are analytically solvable.

Each radial integral is made up of the eigenenergies and Bessel functions, which are integrated to an accuracy of 1 part in 10^{-12} by a Gaussian integration routine. In order that computer time for these calculations is not prohibitive, some skillful storage and handling routines are necessary. The angular factors alone, involving sums over Clebsch Gordan coefficients, take up significant time.

In some of our calculations we have needed up to 16 000 radial coefficients, and this number increases as M (see section 6 for a definition of M). It should be recalled that despite this we only achieved an accuracy of about 1%, due to truncation of the sum.

Despite these difficulties the calculation has been completed, and it is clear that many more diagrams may now be calculated. The prospect of including the self energy in a correct way makes this an interesting field.

10 ACKNOWLEDGEMENTS

I am grateful to the CSIR for financial assistance in the form of a post gradute bursary.

Many thanks go to my supervisor, Prof R D Viollier, for his guidance and time. Previous students of his, R Buser and Petr Zimak, deserve special thanks. Rolf left behind useful (and bug free) software, and Petr was always willing to explain a subtle/simple point. Rudolph Tegen and Gary Tupper attempted to broaden my knowledge via coursework. Allard Schnabel maintained the Computer centre with German efficiency. Prof J Rafelski always injected excitement (and controversy) into physics, although we still differ on whether space or objects contract. The other postgraduate students provided a stimulating environment for debate (mainly political). I acknowledge ejog's acknowledgements.

The radial integrals have no dependence on the magnetic quantum numbers. The angular integral may be evaluated, giving

$$\int d\Omega\, \chi^{\mu' +}_{k'}(\hat{r})\, Y_{JM}(\hat{r})\, \chi^{\mu}_{k}(\hat{r}) = (-)^{\mu+1/2}\, \hat{j}'\hat{J}\hat{j}/\sqrt{4\pi}$$

$$\times \begin{pmatrix} j' & J & j \\ \mu' & M & \mu \end{pmatrix} \begin{pmatrix} j & J & j' \\ 1/2 & 0 & -1/2 \end{pmatrix} \tfrac{1}{2}\left(1 + (-)^{\ell'+J+\ell}\right). \qquad \text{(A10)}$$

in terms of the 3j-symbols, and $\hat{J} = \sqrt{2J+1}$. This expression contains the angular momentum and parity selection rules. The radial integrals may, after some tedious reduction (Vi 83), be written

$$R^{d}_{n'nm} = -\mathcal{N}^{1}_{m}\, R^{-3/2} \int_0^R j_J(\Omega^{d}_{m} r)\, S_{n'n}(r)\, r^2\, dr \qquad \text{(A11)}$$

$$R^{\ell}_{n'nm} = -\mathcal{N}^{\ell}_{m}/\Omega^{\ell}_{m}\, R^{-3/2} \int_0^R \Big[\{ \Omega^{\ell}_{m} r\, j_{J+1}(\Omega^{\ell} r) \qquad \text{(A12)}$$

$$- J\, j_J(\Omega^{d}_{m} r) \}\, U_{n'n}(r) + (K'-K)\, j_J(\Omega^{d}_{m} r)\, T_{n'n}(r) \Big] r\, dr$$

$$R^{\mu}_{n'nm} = \frac{K'+K}{\sqrt{J(J+1)}}\, \mathcal{N}^{\mu}_{m}\, R^{-3/2} \int_0^R j_J(\Omega^{\mu}_{m} r)\, T_{n'n}(r)\, r^2 dr \qquad \text{(A13)}$$

$$R^{\varepsilon}_{n'nm} = \mathcal{N}^{\varepsilon}_{m}\, R^{-3/2} \left(\sqrt{J(J+1)}\,\Omega^{\varepsilon}_{m}\right)^{-1} \int_0^R \Big[J(J+1)\, j_J(\Omega^{\varepsilon}_{m} r) \qquad \text{(A14)}$$

$$\times\; U_{n'n}(r) + (K'-K) \{ J\, j_J(\Omega^{\varepsilon}_{m} r) - \Omega^{\varepsilon}_{m} r\, j_{J-1}(\Omega^{\varepsilon}_{m} r) \}\, T_{n'n}(r) \Big] r\, dr .$$

where the radial functions S, T, and U are given by

$$S_{n'n} = g_{n'} g_n + f_{n'} f_n$$

$$T_{n'n} = g_{n'} f_n + f_{n'} g_n$$

$$U_{n'n} = g_{n'} f_n - f_{n'} g_n . \qquad \text{(A15)}$$

f and g are the quark radial wavefunctions.

REFERENCES

Ba 84 - T Barnes, Phys Rev D30 1961 (1984)

Ba 85 - R M Baltrusaitis, Phys Rev D32 2883 (1985)

Be 74 - C Becchi, A Rouet, R Stora, Phys Lett 52B 344 (1974)

Be 76 - C Becchi, A Rouet, R Stora, Ann Phys 98 287 (1976)

Be 82 - Quantum Electrodynamics, V B Berestetskii, E M Lifshitz, L P Pitaevskii, Pergamon Press (1982)

Bl 50 - K Bleuler, Helv Phys Acta 23 567 (1950)

Bu 83 - R Buser, Ph.D Thesis, Quantum Chromodynamics inside a Cavity, University of Basel, (1983)

Bu 86 - R Buser, R D Viollier, P Zimak, Canonical Quantization and Chromodynamics in a Spherical Cavity, UCT-TP 72/86, (1986)

Ca 78 - R H Capps, Phys Rev D18 845 (1978)

Ca 83 - C E Carlson, T H Hansson, C Peterson, Phys Rev D27 1556 (1983)

Ch 74 - A Chodos, R L Jaffe, K Johnson, C B Thorn, V F Weisskopf, Phys Rev D9 3471 (1974)

A Chodos, R L Jaffe, K Johnson, C B Thorn, Phys Rev D10 2599 (1974)

Cl 79 - An Introduction to Quarks and Partons, F Close, Academic Press (1979)

Cl 80 - F E Close, R R Horgan, Nucl Phys B164 413 (1980)

de 63 - J J de Swart, Rev Mod Phys 35 916 (1963)

De 75 - T DeGrand, R L Jaffe, K Johnson, J Kiskis, Phys Rev D12 2060 (1975)

Do 83 - J F Donoghue, H Gomm, Phys Rev D28 2800 (1983)

Fa 67 - L D Fadeev, V N Popov, Phys Lett 25B 29 (1967)

Fe 71 - Quantum Theory of Many Particle Systems, A L Fetter, J D Walecka, McGraw-Hill (1971)

Fl 84 - M Flensburg, C Peterson, L Skold, Z Physik C22 293 (1984)

Fr 73 - M Fritsch, M Gell-Mann, H Leutwyler, Phys Lett 47B 365 (1973)

Fr 84 - M Frank, P J O'Donnel, Phys Rev D29 921 (1984)

Fr 85 - M Frank, P J O'Donnel, Phys Rev D32 1739 (1985)

Ge 51 - M Gell-Mann, F Low, Phys Rev 84 350 (1951)

Ge 64 - M Gell-Mann, Phys Lett 8 214 (1964)

Ge 86 - M Z I Gering, W D Heiss, Phys Rev D33 1980 (1986)

- Dynamic Interactions in many fermion systems and their effect within the quark bag model, M Z I Gering, Ph.D thesis, University of the Witwatersrand (1986)

Go 57 - Proc Roy Soc (London) A239 267 (1957)

Go 86 - S N Goldhaber, R L Jaffe, T H Hansson, Nuc Phys B277 674 (1986)

Gr 73 - D J Gross, F Wilczek, Phys Rev Lett 30 1323 (1973), Phys Rev D8 3635 (1973)

Gr 74 - D J Gross, F Wilczek, Phys Rev D9 980 (1974)

Gu 50 - S N Gupta, Proc Phys Soc A63 681 (1950)

Ha 83 - T H Hanson, R L Jaffe, Phys Rev D28 882 (1983)

Ha 84 - Quarks and Leptons, F Halzen, A D Martin, John Wiley and Sons (1984)

Is 76 - N Isgur, Phys Rev D13 122 (1976)

Ku 79 - T Kugo, I Ojima, Suppl Prog Theor Phys 66 1 (1979)

Le 79 - T D Lee, Phys Rev D19 1802 (1979)

My 84 - F Myhrer, J Wroldsen, Z Physik C25 281 (1984)

Po 73 - H D Politzer, Phys Rev Lett 30 1346 (1973)

Sc 68 - L I Schiff, Quantum Mechanics, McGraw Hill (1968)

tH 71 - G 'tHooft, Nucl Phys B33 173 (1971), B35 167 (1971)

Vi 83 - R D Viollier, S A Chin, A K Kerman, Nuc Phys A407 269 (1983)

Wr 84 - J Wroldsen, F Myhrer, Z Physik C25 59 (1984)

Ya 54 - C N Yang, R L Mills, Phys Rev 96 191 (1954)

Zi 86 - P Zimak, Quantum Chromodynamics in a Cavity, Ph.D thesis, University of Cape Town, (1986)